UNIVERSITÉ LIBRE DE BRUXELLES

BRUFACE BRUSSELS FACULTY OF ENGINEERING

VRIJE UNIVERSITEIT BRUSSEL

State of health mapping for commercial NMC batteries with hybrid operating conditions

Karthik Prakash

Master thesis submitted under the supervision of
Prof Dr Maitane Berecibar

The co-supervision of
Dr Md Sazzad Hosen

In order to be awarded the Master's programme in
Electromechanical Engineering major in Sustainable Transport and Automotive Eng

Academic year
2022-2023

Consent form for publicising Master's thesis

Student:	Karthik Prakash
Enrolment number :	0583560
Study programme :	Masters in Electromechanical Engineering - STAE
Academic year:	2022-2023
Master's thesis Title:	State of health mapping of commercial NMC batteries with hybrid operating condition
Supervisor:	Dr. Md Sazzad Hosen

Any Master's thesis for which the student has obtained a credit, and for which no non-disclosure agreement (NDA) was drawn up, can be included at no charge in the Vubis catalogue of the central university library as long as the student has given their prior explicit consent.

In the context of the possibility of making their Master's thesis available free of charge, the student chooses one of the following options:

- ☐ OPEN ACCESS: worldwide access to the full text of the Master's thesis
- ☐ ONLY FROM THE CAMPUS: access to the full text of the Master's thesis is only possible from the VUB network
- ☐ EMBARGO FOLLOWED BY OPEN ACCESS: worldwide access to the full text of the Master's thesis only after a specific date, namely .....
- ☐ EMBARGO FOLLOWED BY ACCESS ONLY FROM THE CAMPUS: access to the full text of the Master's thesis only from the campus and only after a specific date, namely .....
- ☒ FULL TEXT NEVER ACCESSIBLE: no access to the full text of the Master's thesis
- ☐ NO PERMISSION to make accessible

The supervisor confirms acknowledgement of the intention of the student to make the Master's thesis available in the Vubis catalogue of the central university library.

Date: 30.05.2023
Signature of supervisor: Sazzad

This document will be included in the Master's thesis. Any student who fails to include the document in their Master's thesis and/or has failed to indicate a choice and/or has failed to sign the document and/or has failed to inform the supervisor will be considered as not having granted permission to make their thesis public; in that event, the Master's thesis will only be archived and will not be accessible to the public.

Drawn up at ...Brussels, Belgium..... on 01-06-2023.....

Karthik

Signature of student

Abstract

Currently, numerous studies are being conducted in the field of battery technology, with a huge emphasis given to the ageing of batteries. Among batteries, Li-ion battery is most often used in electric vehicle technology as it has several advantages. Many models are being developed to understand how Li-ion batteries degrade over time. In real-life applications, the operating conditions are quite different from the laboratory operating conditions. Hence, a model that can estimate the Li-ion battery deterioration for the same battery chemistry (such as NMC.) matching real-life scenarios is necessary.

The main objective of this thesis is to investigate five different commercial Li-ion batteries that come under NMC chemistry. To make the experiment closer to the practical scenario, a hybrid testing methodology that combines cycling and rest periods in a single round is followed. Once the experiment is done, the data is analyzed, and the behaviour of parameters – internal resistance and capacity over a period of several cycles are observed while keeping in note other parameters such as SoC, voltage, current and temperature. The parameters of internal resistance and capacity are chosen as they are crucial in determining the degradation of the battery. Next, to estimate these two parameters, a fourth-order polynomial equation is formulated to closely represent the behaviour of these parameters using the curve fitting method in Microsoft Excel. This is then validated using MATLAB curve fitting toolbox. Once verified, the formula can be used to estimate internal resistance and capacity, and thus provide a simple and accurate way of determining battery deterioration that closely fits actual practical situations.

Acknowledgements

First, I thank my supervisor Prof Dr Maitane Berecibar, for her valuable input as well as this opportunity to work on this topic. Next, I thank my co-supervisor Dr Md Sazzad Hosen for his regular guidance. I am very grateful to him because I could reach him whenever I had doubts which he patiently clarified. I extend my gratitude to the Battery Innovation Centre (BIC) department for their involvement. Finally I thank my family members and friends for their love and motivation.

Contents

List of Figures

List of Tables

List of Abbreviations

SoH	State of health
SoC	State of charge
DoD	Depth of discharge
OCV	Open circuit voltage
IR	Internal resistance
BMS	Battery management system
BoL	Begining o life
EoL	End of life
NMC	Nickel Manganese Cobalt
EV	Electric vehicle
GHG	Green house gases
ICE	Internal combustion engine
CCCV	Constant current constant voltage
SEI	Solid electrolyte interphase
Ah	Ampere hour
HPPC	Hybrid pulse power characterization
WLTC	Worldwide harmonised Light duty driving Test Cycle
FEC	Full equivalent cycle
CEI	Cathode-electrolyte interphase

Chapter 1

General Introduction

1.1 Background

Electric vehicles (EVs) are becoming highly significant as they mostly rely on renewable energy sources instead of fossil fuels. The ongoing trend in EV sales can be noticed in fig.1.1, based on which it can be easily seen that the market for EVs is increasing. For instance, 2021 showed a tremendous growth rate of 108 % for EVs. Over one-third of these sales occurred in the European Union (EU) region alone. Considering the overall global trade accounted for 9% of automobile sales worldwide, EVs have vast and immense potential in the future commercial market [2].

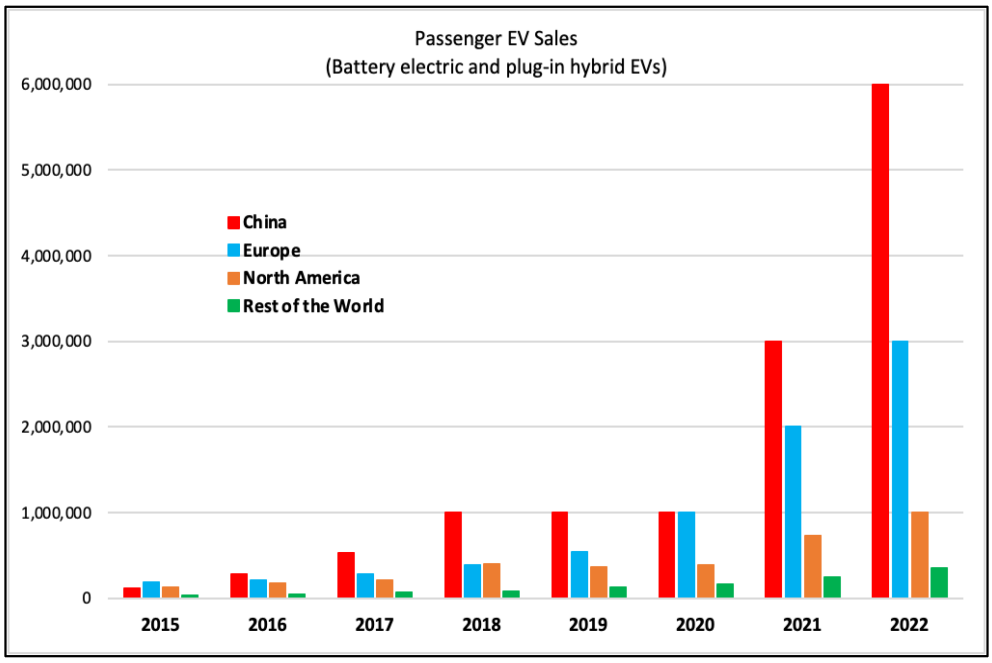

Figure 1.1: Ongoing EV sale trend [2].

The main benefit of Electric vehicles compared to conventional fossil fuel is that the emission is very low. On average, EVs emit significantly less Green House Gases (GHG) compared with, as seen in Fig. 1.2.

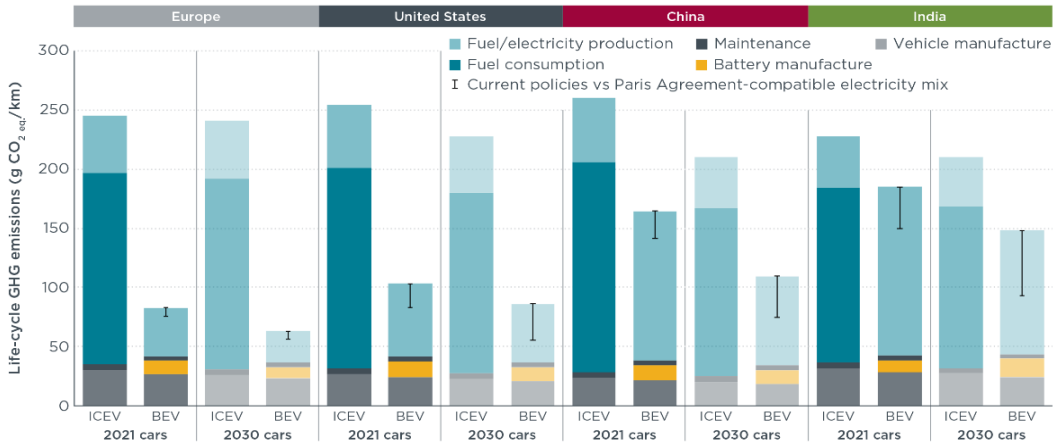

Figure 1.2: Comparing GHG Emissions of Internal Combustion Engines (ICEs) and Battery Electric Vehicles (BEVs) [7].

In the case of an Electric Vehicle, the battery is the key integral part, accounting for energy storage and shaping the main characteristics of EVs, such as lifetime, range of driving, acceleration power and thermal constraints. Apart from this, they also influence the cost of EVs [1]. There are many types of batteries classified based on their chemical composition. Among these, Lithium-ion is the most popular choice, and most EVs use them. Some other examples include Nickel – Cadmium, Lead acid, Nickel -Iron etc. [2]. This is because apart from the low maintenance required for Li-ion batteries, the element- lithium has low weight resulting in high energy density [3].

1.1.1 General structure of Li-ion battery

The general structure of a Li-ion battery is shown in fig.1.3
The main parts of the battery are[5]:

- **Cathode:** The positive electrode determines the battery's capacity and power output.
- **Anode:** The negative electrode decides the battery's life cycle, charging rate, and safety.
- **Electrolyte:** Electricity conducting liquid where exchange of ions takes place.
- **Separator:** This film separates anode and cathode. It is made from a porous polymeric substance. The exchange of ions takes place through this layer.
- **Current Collector:** Current conductors at anode and cathode terminals used for the connections.

Li-ion batteries produce current when Li-ion moves between the cathode and anode. During charging, Li-ions move from cathode to anode, and while discharging, the movement of Li-ions is from anode to cathode.

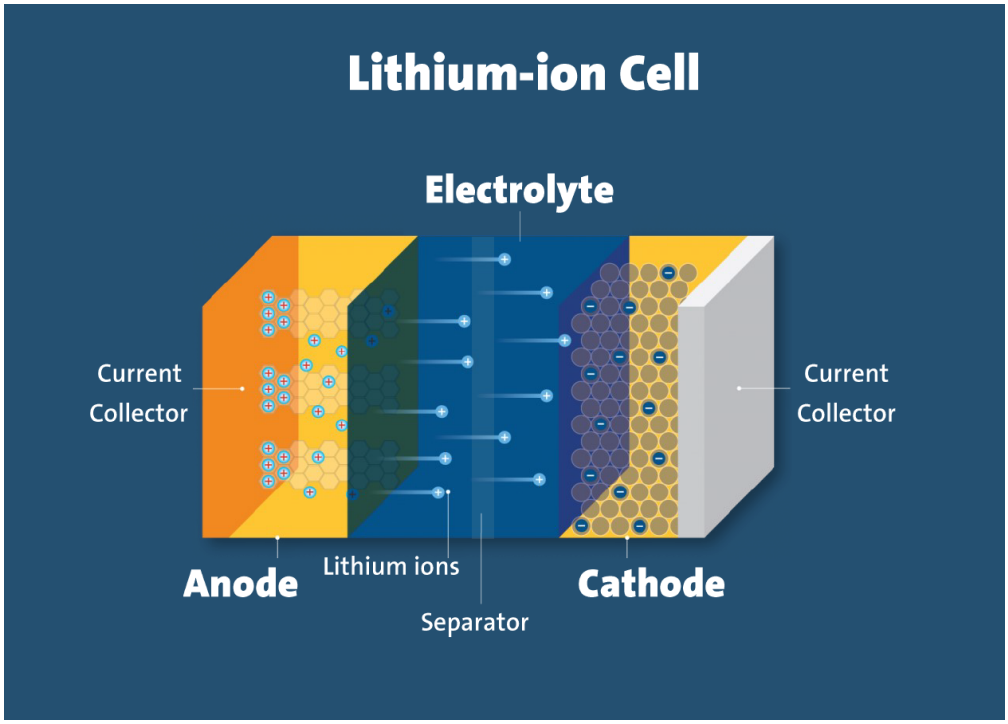

Figure 1.3: General structure of Li-ion battery[5].

The main concern with these types of batteries is ageing. Many factors contribute to the degradation of batteries, including both external and internal; due to this, the prediction of ageing behaviour is very complicated and challenging. During the lab test scenario, main focus is given to the charging and discharging cycle, but it's not the same as the real world. While driving, the electric vehicle will go through charging, discharging and idle phases [14]. Together, these factors contribute to cycle and calendar ageing, leading to a loss in capacity and increased resistance. Therefore, accurate mapping of the State of Health (SoH) under actual scenarios will give information on how these batteries act inside the car under real driving conditions, allowing us to predict cell degradation with good accuracy and the effect of different factors. Some of these factors which contribute towards the degradation of batteries are both external and internal temperature, charging and discharging rate, state of charge(Soc), mechanical stress, depth of discharge (DoD).

1.2 Battery terms and parameters

This section briefly describes important terms for understanding battery performance.

- **State of Health (SoH):** SoH indicates battery capacity as shown in equation.1.1 where Q is the present capacity of the battery in Ah, Q_0 is the original capacity in Ah.

$$SoH = (\frac{Q}{Q_0}) * 100 \tag{1.1}$$

- **State of Charge (SoC):** SoC is the charge level in a battery. This is the most common parameter a user is familiar with.

- **Open Circuit Voltage (OCV)**: The OCV of a battery cell is defined as "the potential difference between the positive and negative terminals when no current flows and the cell is at rest".

- **Internal Resistance**: The internal resistance of the battery refers to opposition to flow of electrons through it. As the battery reaches the end of life, the internal resistance of the battery will rise as a result of a voltage drop and increase in temperature.

- **Capacity fade**: The capacity fade in the battery is a measure of reduction in battery capacity over a period of time as shown in equation.1.2. where Q_0 is the initial battery capacity in Ah, Q_n is capacity remaining in the battery after use.

$$CF = (\frac{Q_0 - Q_n}{Q_0}) * 100 \tag{1.2}$$

- **Specific energy**: Specific energy of battery stands for its capacity in weight - Wh/kg.

- **Specific power**: Specific power of battery stands for its power density which is measured in Watts per kilogram (W/kg).

- **Specific capacity**: Specific capacity of a cell stands for the amount of charge in mAh it can deliver per gram of material.

- **Battery Management System (BMS):** The primary function of BMS is to indicate the SoC of the battery and send alarm signals in critical situations like temperature exceeding rated permissible levels. However, it can also perform additional functions such as giving signs of SoH, end of life etc.

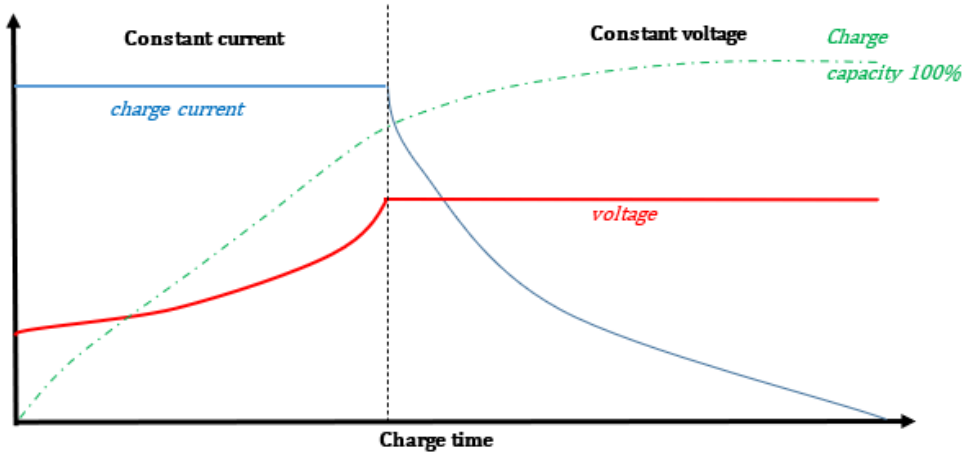

Figure 1.4: Graph showing CCCV charging[19].

- **Constant Current (CC):** In this method, battery charging is done with the current kept constant. The main purpose of this method is to avoid overcurrent. However, this method can also be used to stop overvoltage by using low constant current values
- **Constant Voltage (CV):** In this method, battery charging is done with the voltage kept constant. The main purpose of this method is to avoid overcharging. However, this method can also stop high-temperature rise by using initial low voltage and then slowly increasing it.
- **Constant Current Constant Voltage (CCCV):** In this method, depending on the voltage level of the battery, charging switches between CC and CV mode. This is the most commonly used charging method in Li-ion batteries.

1.3 Battery ageing

Typically, a battery is said to reach its end of life at 80% of its rated capacity. A more precise way of describing the end of life of a battery is when it has lost more than 20% of its initial capacity and has a 100% increase in internal resistance [15]. There are two types of ageing - cycling ageing and calendar ageing.

- **Cycling ageing**: Deterioration of battery with time due to using it is called cycling ageing. It is named so because the battery undergoes several charging and discharging cycles. At reduced temperature and high charge rate, a coating starts forming at the anode. This is one of the leading causes of cycling ageing. However, under unusual circumstances like abnormal current rate and sharp discharges, collector corrosion and particle cracking can lead to cycling ageing. [12].
- **Calendar ageing**: Deterioration of battery with time when it is at rest - as in when stored is called calendar ageing. Built-up of Solid electrolyte Interphase (SEI) at the anode is the primary cause of calendar ageing. This typically occurs at high temperatures and high SoC. [12].

The factors contributing to ageing can be classified as internal and external factors. Internal factors are chemical reactions occurring at the anode and cathode terminals. External factors are a phenomenon that occurs outside the battery, such as the impact of temperature. As shown in Fig. 1.5, formation of Solid electrolyte interphase (SEI) film at the electrode, destruction of the electrode structure, deposition of lithium, and phase change of electrode material are some reactions that contribute to battery ageing [10].

1.3.1 Anode aging mechanisms in Li-ion battery

Formation of Passivated Surface Layer is one main factor behind anode ageing. Solid electrolyte Interphase (SEI) is a layer made by substances like CO_2OLi and $ROCO_2Li$ that are formed when the anode of a Li-ion battery reacts with an electrolyte solution. The anode material in the battery is usually graphite. The electrolyte is organic, for instance, $LiPF_6$. Oxidation of graphite anode occurs when lithium ions intercalate into the lattice structure of the anode. This happens at higher potentials of battery. Consequently, chemical reactions occur between the highly reactive co-solvents, resulting in products that continue accumulating on the surface of the anode. The continuous responses lead to the isolation of graphite particles. When the battery is under storage conditions, loss of Li-ion occurs due to the surface layer. This eventually

leads to the deterioration of battery properties as pores appear on the anode—also, parameters such as impedance and charge transfer resistance increase.

Another factor that contributes to anode ageing is anode impedance. Anode impedance is the resistance due to the flow of Li-ions due to a passive layer on the anode. As the temperature, cycle number, particle size of anode material and charge rate increase, the anode impedance also increases.

The next point to consider in anode ageing is the reduction of recyclable Li-ions. Over some time during battery operation, Li-ion reacts with water and decomposes electrolyte compounds. This, in combination with SEI, leads to irreversible Li-ion loss. Anode degradation also occurs due to structural changes. Another key factor contributing to anode ageing is the consequences of structural changes. Graphite particles that are not well-oriented result in a low reversible capacity of the anode. This is because of two reasons. The first reason is that Li-ions/electrolytes interact irreversibly when new borders exist in the crystalline structure. The second reason is that the intercalation kinetics of Li become harder. The mechanical strain on the anodes is due to increased SoC and high charging (C) rate. The final disorientation of graphite particles is because of the overall mechanical stress due to reported changes in Li-ion cracks and the breaking of graphite particles. Active surface area increases with a decrease in porosity. This is because the electrical path in graphite decreases as the porosity increases—irreversible capacity. At high temperatures, there is more heat generation in smaller particles than in larger particles due to the exothermic reaction. So the irreversible capacity of graphite is more for smaller particles [11].

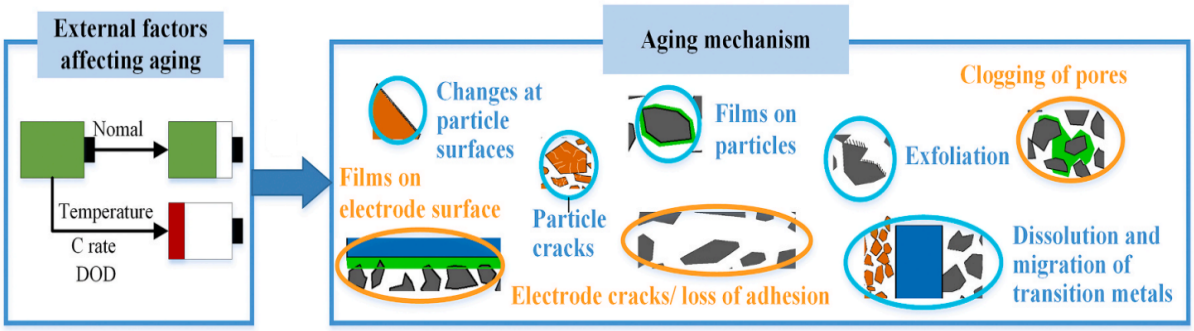

Figure 1.5: Ageing mechanism in batteries [10].

1.3.2 Cathode aging mechanisms in Li-ion battery

One primary factor contributing to the ageing of cathode is the dissolution of cathode materials, as after this, the dissolved products move and deposit at the anode, thus worsening the electrolyte deterioration. Similar to SEI, CEI layer formation also occurs due to the oxidation of electrolytes. But this is not as thick as the SEI layer. However, this adversely impacts the battery capacity along with its reversible capacity. Another factor contributing to cathode ageing is the mixing of cations which eventually reduces battery capacity. Apart from this, over a period of time, materials in the cathode start transitioning, which results in mechanical stress and eventual degradation of capacity [31].

1.4 Types of Li-ion batteries

Different types of Li-ion batteries are classified based on the substance used in the cathode as shown in table 1.1[20]. One of the earliest Li batteries used in the market was Sony's $LiCoO_2$.

Type of battery	Specific Energy	Specific Power	Performance	Lifespan	Safety	Cost
Lithium Nickel Manganese Cobalt oxide	High	Medium	Medium	Medium	Medium	Low
Lithium Titanate	Low	Medium	High	High	High	High
Lithium Iron Phosphate	Low	High	Medium	High	High	Low
Lithium Cobalt Oxide	High	Low	Medium	Low	Low	Low
Lithium Manganese oxide	Medium	Medium	Medium	Low	Low	Low
Lithium Nickel Cobalt Aluminium Oxide	High	Medium	Medium	Medium	Medium	Low

Table 1.1: Comparison of different Li-ion Batteries [20]

Its primary disadvantage was that it was expensive due to a large amount of Cobalt being present in it. Apart from this, it also had a limited capacity of around 155 Ah/kg. In the context of Lithium-ion batteries, mainly three different substances are used at the cathode - specifically, Lithium Nickel-Manganese-Cobalt (NMC) oxide, Lithium-Nickel-Cobalt-Aluminium (NCA) oxide and Lithium Iron Phosphate (LFP) [4]. Among these, NMC batteries are more commonly used as they have less cobalt content [6] and high specific energy. The capacity of NMC batteries is around 160–200 Ah/kg. It also contains less proportion of Cobalt in it [21]. The presence of Manganese in NMC results in the low internal resistance of the battery. In addition to all these, the NMC battery has high capacity from the presence of Nickel [24]. Hence due to these reasons, NMC has turned out to be the most frequently used type of Li-ion battery which can be seen in fig.1.6. In this thesis, for the experiment, all five batteries used are of NMC chemistry.

1.5 Characteristics of Li-ion battery by shape

The shape determines some of the characteristics of Li-ion batteries, such as storage, energy and power density. Based on the shape, there are four types of Li-ion batteries, as shown in fig.1.7 [25].

- **Cylindrical batteries:** Most companies follow a standard cell size while using this shape. Currently, 21700 cells are considered good enough concerning capacity and production ease. The capacity of 21700 cells is 6Ah, and the volume is 97 cubic cm.

- **Prismatic batteries:** In these batteries, electrodes are assembled either by stacking up layers or by 'jelly-rolling'. A further layer of hard plastic or metal is needed to stabilise this structure. The main advantage of this shape is that it occupies space in a more optimum manner. The high cost of manufacture is its demerit.

- **Coin batteries:** Though this shape is very compact, it is not used anymore due to safety issues. Its shape makes it hard to use additional defence appliances with it.

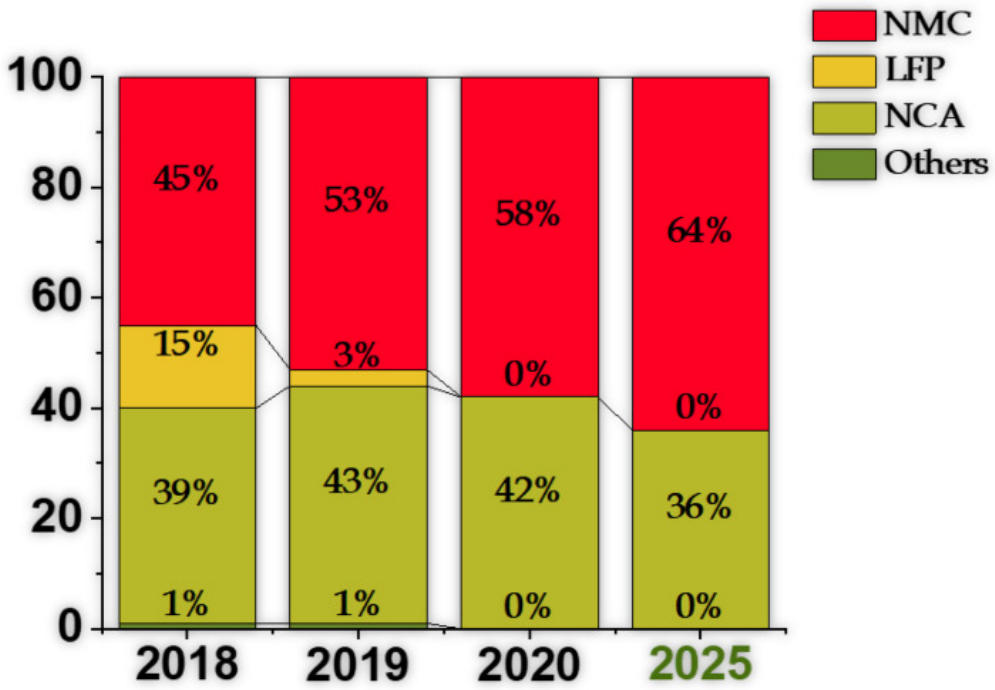

Figure 1.6: Usage of different types of batteries in EVs [4].

- **Pouch batteries:** This is one of the most flexible shapes with a very high packing efficiency of 90% to 95%. It also has the additional merit of having low weight. Its disadvantage is the necessity of extra support.

In the experimental setup, prismatic and pouch cell is used as these are commonly used in commercial uses.

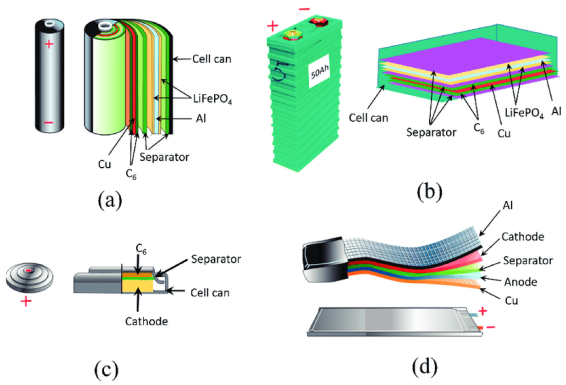

Figure 1.7: Different shapes of Li-ion batteries - (a) is cylindrical, (b) is prismatic, (c) is a coin, (d) is pouch [25].

1.6 Thesis objective and scope

This master thesis will focus on the NMC battery technology of which five different commercial battery cells are investigated. The chosen batteries are 37 Ah, 40 Ah, 43 Ah, 60 Ah and 50 Ah. The batteries are aged by a combination of charge-discharge cycles and rest, and hence this way of testing will be called hybrid testing methodology, the main advantage being that it emulates actual battery usage in transport applications. The experiment comprises of HPPC test, capacity test with WLTC test cycles and operating conditions monitoring SoC, temperature and C-rate.

The thesis will build statistical relations between the usual or newly identified degradation parameters by analysing the gathered dataset. These batteries' fading capacity and growing internal resistance will be checked with measurable parameters such as voltage, current, ambient temperature, etc. The method used for this will be curve fitting using both Microsoft Excel and MATLAB. The polynomial used for modelling will be decided based on how well the experiment data fits it for which, the R^2 value will be used. An empirical model could be proposed for each type of NMC battery the main purpose of the model would be estimating the internal resistance and capacity of the battery. The inferences from the experiment will also help in deciding whether there is a correlation between these two parameters. The final model can be used to predict the lifetime of a battery.

1.7 Outline of thesis

The thesis is structured as follows.

- Chapter 2 describes the different testing methods as well as the experimental method that was used for the thesis.
- Chapter 3 presents the capacity fade and internal resistance calculation and the comparison between the two with respect to rounds.
- Chapter 4 provides the curve fitting results and its analysis
- Chapter 5 contains conclusion, limitation and future work.

Chapter 2

Design of Experiments

2.1 Some common test methodologies

This part of the chapter describes some of the common test cycles and methodologies that are used in battery testing.

2.1.1 Capacity test

The purpose of this test is to estimate the capacity of the battery. This test is essential to estimate energy storage [32]. One way to estimate the battery capacity is the technique of Coulomb counting. In this method, BMS monitors the current every second; current x hours gives the capacity in Ah. The main advantage of this method is that it is conceptually easy and the main disadvantage of this method is that it requires continuous monitoring of current. Another method to estimate capacity is by using the voltage measurement. This works well for low loads such as cell phones but is not suitable for heavy loads. Having a look-up table to estimate the capacity based on already-built voltage profiles works well if parasitic resistance values are also included. A third way to estimate the battery capacity is by combining the first two methods. Initially voltage-based estimation can be used, followed by Coulomb counting [35].

2.1.2 Hybrid Pulse Power Characterization (HPPC) Test

This test subjects the cell at various points of SoC to a sequence of charging and discharging pulses [16]. In this manner, the battery's internal resistance can be calculated [15]. Since the time duration of the pulses is very short, neither the SoC nor OCV of the cell changes [16]. Fig.2.1 shows plots of voltage and current readings from an example HPPC test where brief pulses (duration of 10 seconds) of discharge and charge are applied at several SOC points, with each point varying by 10%.

$$IR = \frac{V_2 - V_1}{I} \tag{2.1}$$

The equation 2.1 calculates the internal resistance. V_1 and V_2 are the instantaneous voltage between two points with a time difference of 10 Sec. I is the current measured at the desired C rate.

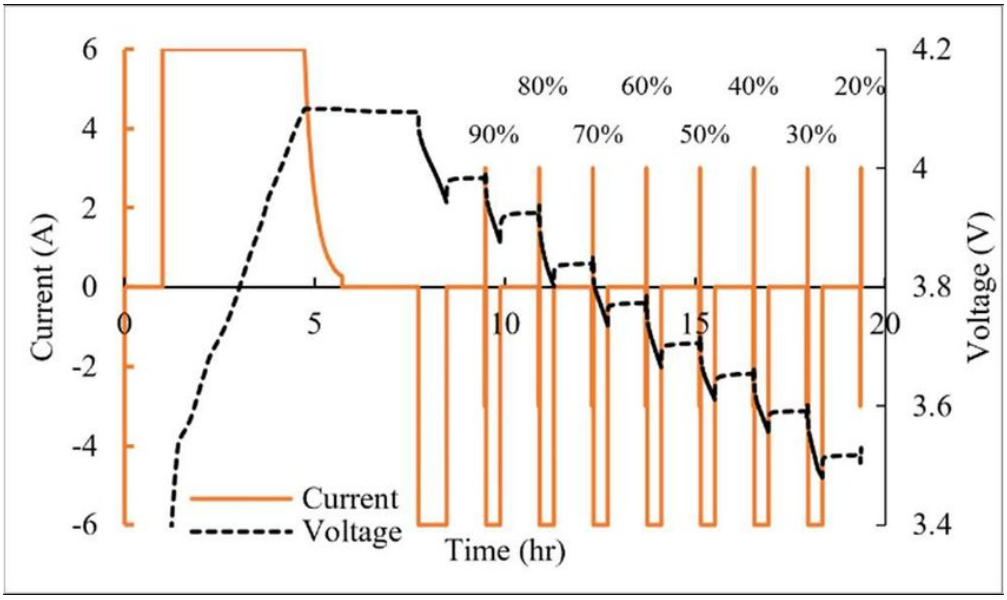

Figure 2.1: Plot from an example HPPC test [16].

2.1.3 Cycle life test

In the cycle life test, the battery performance is analysed after being subjected to various cycles of charge and discharge to replicate a scenario that is being used in an actual application. During this test, other parameters, such as charging rate and cycle duration, are predetermined. Cycle life testing often consumes a considerable amount of time, and now there are a lot of ongoing studies to optimise this testing methodology [33].

2.1.4 Calendar aging test

The calendar ageing test aims to subject the battery to various storage conditions that are pre-planned, such as already fixed humidity and temperature, to study how it degrades over a period of time when it is not in use [34].

2.1.5 Worldwide harmonised Light duty driving Test Cycle (WLTC):

WLTC is a test cycle for light duty vehicles developed by the Forum for the Harmonisation of Vehicle Regulations (WP.29) of the United Nations Economic Commission for Europe (UN-ECE) to represent general driving characteristics in various countries. Since different countries have average speeds that differ vastly, WLTC cycle is based on speed class and not based on the classification of roads (such as rural or urban). Hence currently, based on speed, there are four catergories of WLTC - low, medium, high and ex-high [13].

- Low speed: less than 50 km/h
- medium speed: less than 70 km/h
- high speed: less than 110 km/h
- ex-high speed: more than 110 km/h

2.1.6 Hybrid test methodology

A hybrid testing method combines cycling and resting into a single round [14]. This type testing methodology is more practical. It resembles a real driving behavior of an electric vehicle on a trip. Initially, it undergoes periods of charging and discharging as the driver wants during the trip. Once the vehicle is parked for extended periods after the trip, it is stationary and is thus at rest. Hence, this test methodology provides a combined effect of cycle and calendar ageing, which can be replicated in the normal lab test. The results obtained from these types of tests will have more similarity towards the actual driving behavior. Many researchers have created there on testing procedures by varying different conditions. In this type of ageing tests, there are two rest periods: the first is between charging and discharging, and the second is after a complete cycle.

2.2 Used experimental protocol

The experimental setup uses five batteries: NMC 37, 40, 43, 50 and 60 (where the number stands for battery capacity in Ah). NMC 37, 43 and 50 are prismatic, whereas NMC - 40 and 60 are of pouch shape. NMC is the cathode in all these batteries, and graphite is the anode. These technical details are indicated in the table 2.1.

Type	Prismatic	Pouch	Pouch	Prismatic	Prismatic
Rated Capacity	43Ah	40Ah	60Ah	37Ah	50Ah
Nominal Voltage	3.6V	3.7V	3.7V	3.65V	3.6V

Table 2.1: Technical specifications of cells used

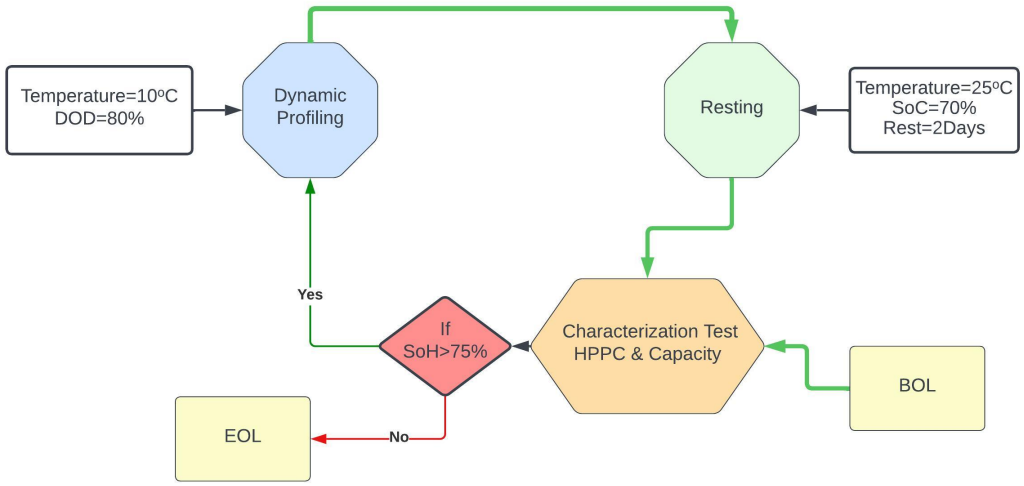

Figure 2.2: Schematic representation of Experiment

The experiment is designed in such a way that it includes different stress factors and varying operational conditions. The primary reason for including dynamic profiling and resting phases is to recreate a driving scenario in the real world. The experiment is carried out as follows: [14].

- The experiment starts with the characterisation test, comprising a capacity check and an HPPC test; these tests aim to measure the capacity and the resistance after each round. Before beginning rounds, the cells are subjected to charge (CCCV during charging) and discharge (CC during discharging) cycles to turn on ions and verify that the electrical connection is fine. This is followed by checking the characteristics of cells using a capacity check. This test is done at room temperature, where the batteries are subjected to charge cycles and discharge at rated current C/3 rate. The capacity measured at the beginning

is called BoL capacity, which is the reference to calculate the State of Health after each round. After each round, the State of Health can be calculated using the equation2.2. Fig2.3 depicts the curve of discharge capacity vs total time

$$SoH = \frac{Actual\ capacity\ or\ IR}{Measured\ capacity\ or\ IR}. \tag{2.2}$$

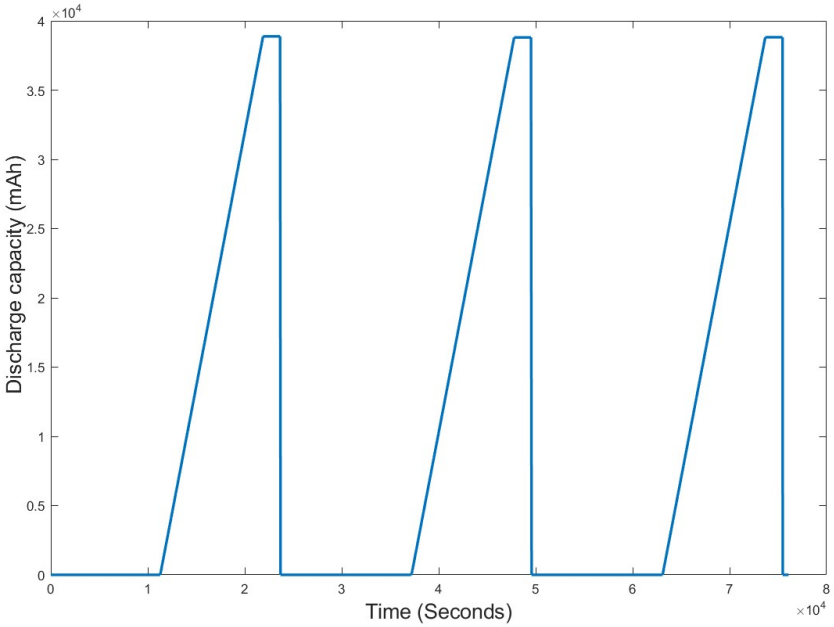

Figure 2.3: Discharge capacity curve of NMC 40Ah

- The next test under the characterisation category is the HPPC test which stands for Hybrid Pulse Power Characterization; the main aim of this test is to find the internal resistance after each round; under this test, the cell undergoes a series of high power pulses which are at different duration and intensities which is followed by a rest time. In this test, the C rates used are 0.33C, 0.5C and 1C, and the SoC chosen are 80%, 50% and 20%. Using the nominal value and the actual value, variation in the value of resistance can be obtained. Resistance calculated at 80% SoC with C/2 discharge pulse is used for reference for all the calculations. The rest time is 10 mins. Fig. 2.4 and fig. 2.5 shows the current and voltage curves during the HPPC test of NMC 50Ah at the beginning of life.

- Next is the dynamic profiling test; in this case, a worldwide harmonized light-duty test cycle (WLTC) is done at 10 °C with the starting SoC at 90% and the Depth of discharge for each cycle being 80%. Prior to the measurement of internal resistance and capacity, this procedure was continued for 12 days. The current calculation for WLTC test was done using the equation2.3[14] Here, all the calculations are done based on Audi e-tron, where M is the vehicle weight 2490kg, S is the frontal area $2m^2$,v is the velocity of the vehicle, C_x is the drag coefficient 0.32, g is the gravitational constant 9.81m/s^2, η is the efficiency of gearbox 0.9, Φ is 0.01, a is the acceleration, V is the voltage of battery pack. Only

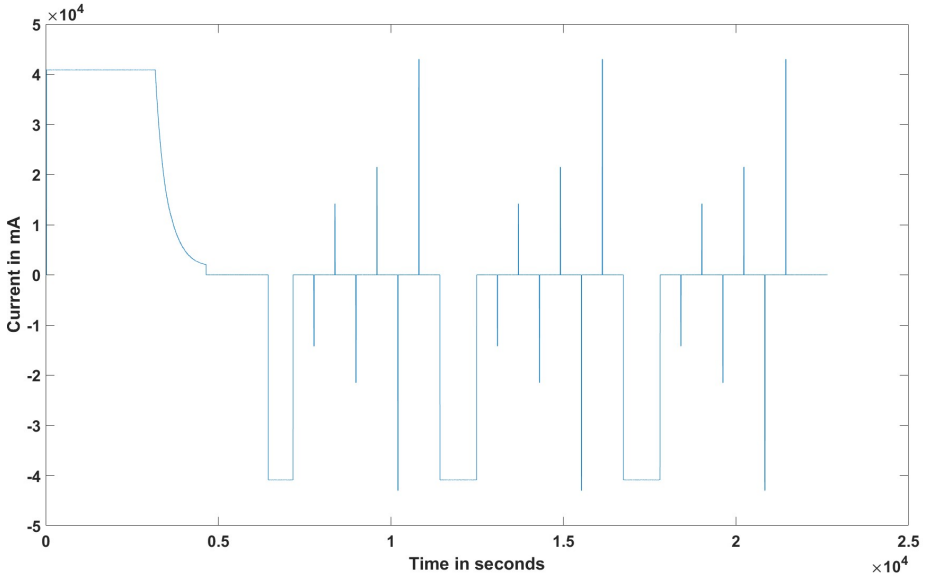

Figure 2.4: HPPC-Current curve of NMC 43 Ah

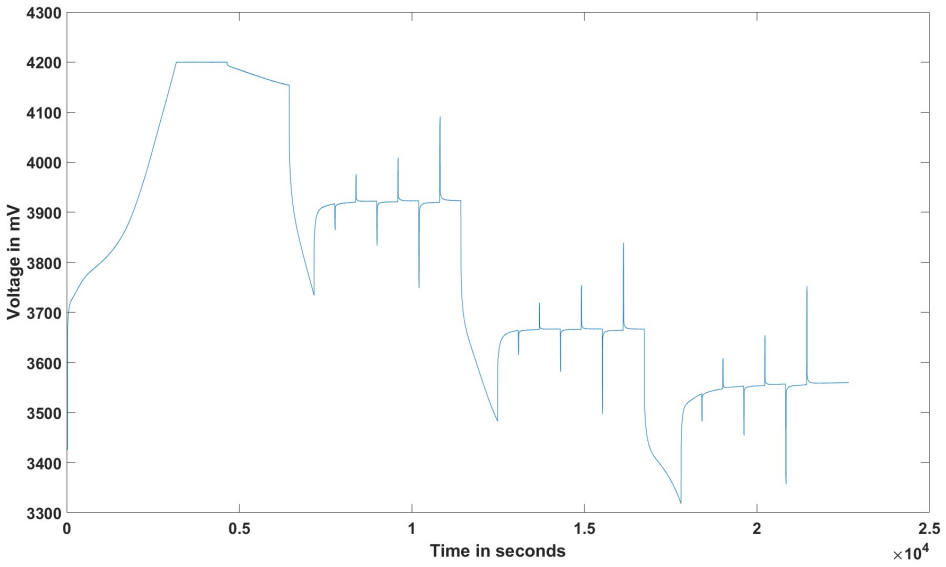

Figure 2.5: HPPC-Voltage curve of NMC 43 Ah

the sub-urban portion of WLTC currents is used in the experiment this is adjusted based on the cell level. Figure 2.6 shows the dynamic profile for one hour. After the dynamic profile testing, the cells are kept in the relaxation phase for 2 days, where the temperature is maintained to 25°C at an SoC of 70%. The main aim of the relaxation phase is to stimulate calendar ageing.

$$I = \frac{0.5 * \rho * S_{cx} * v^3 + \Phi * M * g * v + M * a * v}{V * \eta}. \tag{2.3}$$

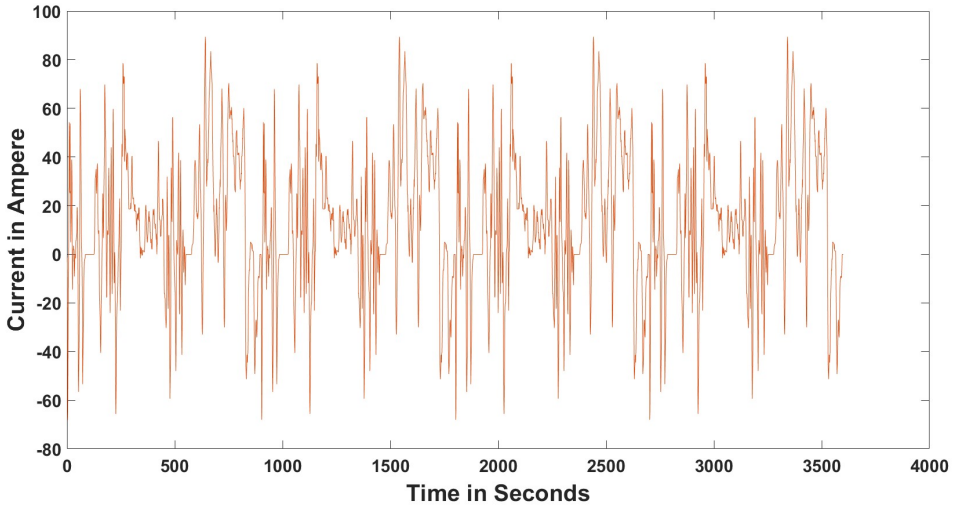

Figure 2.6: Dynamic Profiling for one hour

- If the SoH is less than 75 % then the cells are said to be at the End of Life (EoL). In order to confirm EoL, the cells once again undergo characterisation tests. Once confirmed, it is either stored or disposed of safely.

Chapter 3

Result & Analysis

This chapter contains the results and analysis of the experiment carried out in this thesis. Table 3.1 depicts the full equivalent cycles for the number of rounds. In the table 3.1 regarding NMC 43Ah, after the second round the number of cycles is declining drastically. This can be caused due to several reasons like battery issues, contact problems between the terminals, and contact resistance. Since the number of commercial cells available for the testing was limited, the test was continued with the same cell until round 6. In case of NMC 50 Ah and NMC 40 Ah the test continues smoothly for 11 rounds whereas for NMC 37 Ah there are 7 rounds. NMC 60 Ah has just 5 rounds. Unlike NMC 43 Ah, there is a sufficient number of FEC between the rounds of the other four cells, indicating that the test was successful.
Full Equivalent Cycle (FEC) is a cycle counter that indicates the total Ah throughput in a CCCV charging based on the nominal capacity. FEC compares all cycle outcomes independent of the actual cycle numbers [1].

3.1 SoH based on capacity fade

The capacity was measured after each round at room temperature using the CCCV-CC test cycling method. The C/3 rate is taken as the standard point for calculating the SoH (cap) in each round. The SoH (cap) at each round is calculated by using the equation 3.1. Figure 3.1, 3.2, shows the current, voltage and discharge profile which is used for the capacity estimation in the case of NMC 50Ah at round 1. Table 3.2 shows the variation in the capacity of different cells based on round.

$$SoH_{cap} = \frac{Measured\ capacity\ \sout{in\ each\ round}}{BoL\ Capacity} * 100\%. \tag{3.1}$$

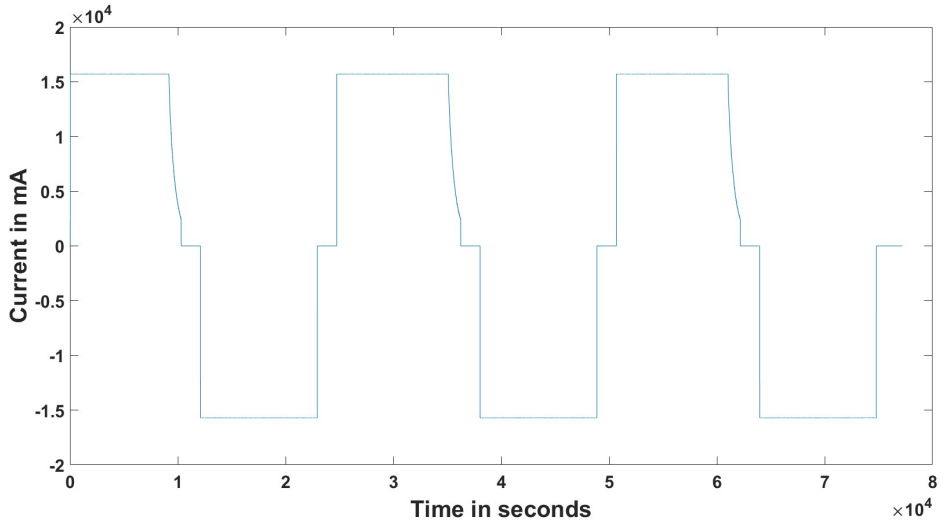

Figure 3.1: Current profile of NMC 50 Ah during first round

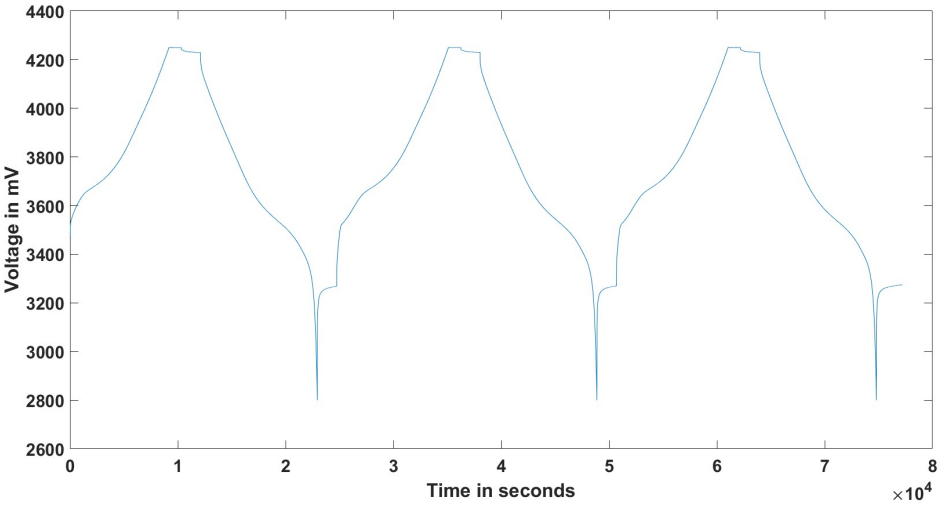

Figure 3.2: Voltage profile of NMC 50 Ah during first round

	Full Equivalent Cycles (FEC)				
Rounds	**NMC 50Ah**	**NMC 43Ah**	**NMC 40Ah**	**NMC 37Ah**	**NMC 60 Ah**
0	0	0	0	0	0
1	87	96	36	101	142
2	174	177	123	202	230
3	248	195	209	286	320
4	304	202	312	387	333
5	392	209	415	472	433
6	480	214	519	563	
7	568		623	659	
8	634		714		
9	669		755		
10	757		858		
11	845		961		

Table 3.1: Number of Full Equivalent Cycles (FEC) for each round

Rounds	**NMC 50Ah**	**NMC 43Ah**	**NMC 40Ah**	**NMC 37Ah**	**NMC 60Ah**
0	100	100	100	100	100
1	99.26	92.89	100.01	98.09	98.16
2	99.06	88.07	100.20	97.84	96.19
3	98.84	85.11	100.30	97.06	92.82
4	99.00	84.20	100.46	93.81	86.62
5	98.52	82.63	100.26	88.80	65.49
6	98.14	81.04	99.96	83.32	
7	97.87		99.67	77.08	
8	97.73		99.94		
9	97.57		99.83		
10	97.65		99.72		
11	97.39		99.28		

Table 3.2: SoH_{Cap} variation in percentage for different cells depending on the rounds

Figure 3.3 shows the SoH_{Cap} for different cells based on the full equivalent cycle, which depicts the variation in the SoH_{Cap}. In contrast, the X-axis shows the full equivalent cycles and Y axis shows the variation in SoH_{Cap}. The graph shows that NMC 50Ah and NMC 40Ah follow the same trend but NMC 43Ah, NMC 37Ah, and NMC 60Ah behave similarly. Further investigation of these trends shows that these five commercial cells can be grouped into two groups based on the cell property. Power-optimized cells and high-energy cells, NMC 40Ah and NMC 50Ah are Power-optimized cells, whereas NMC 43Ah, NMC 37Ah and NMC 60 Ah are high-energy cells[37][38].

Depending upon the application, Li cells can be of high-energy-density cells or high-power-density cells. In this experiment, two categories of cells are used - high energy density cells and optimised high power cells that can withstand high charge and discharge rates.

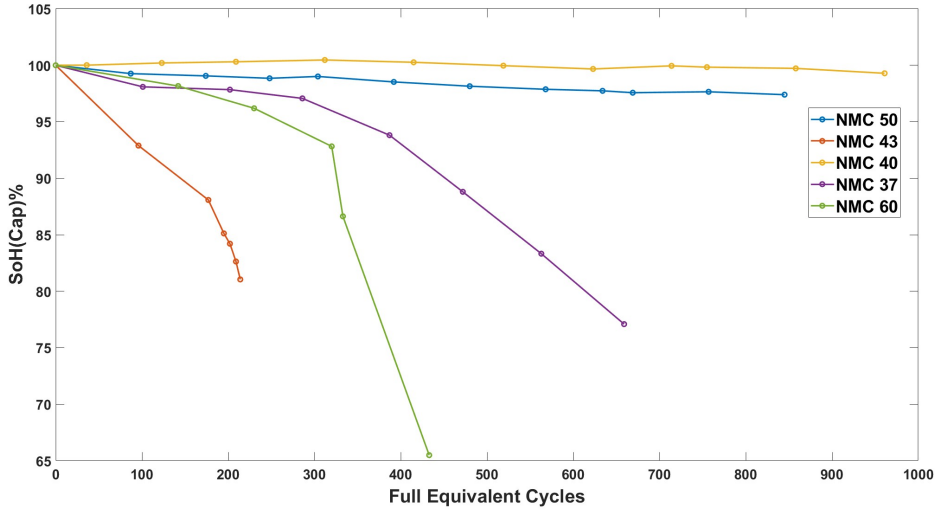

Figure 3.3: SoH_{Cap} in different cells

In the case of a power-optimized cell, the capacity value almost remains constant throughout the experiment cycle. In the case of high energy cells, we can see the knee points after the second round for NMC 43Ah, whereas in the case of NMC 60Ah and NMC 37Ah, knee points are after the third round. In the case of battery degradation, the Knee point is the point at which the capacity fade starts to decline rapidly [36]. The importance of the knee factor is that it can be used to estimate when the battery needs to be changed as its capacity starts to decrease. Hence knee factor is a crucial parameter for developing precise battery models. After the knee point, all three cases' capacity declined drastically. In the case of NMC 60Ah, the SoH dropped below 70% after FEC 443, whereas NMC 37Ah and NMC 43Ah have a SoH of 77% and 81%, respectively. From Figure 3.3, it can be seen that optimised high power-density cells have higher capacity than high energy-density cells, whose capacity starts declining sharply after the knee point. This is primarily because high energy-density cells generate more heat because they have higher internal resistance, resulting from their structure comprising thinner current collectors and thick active material layers [28].

3.2 SoH based on internal resistance growth

Internal resistance is calculated using the HPPC method. Battery cells are subjected to high power pulses for 10s for different C rates at various values of SoC. The C rates used are 0.33C, 0.5C and 1C, whereas the values of SoC are 80%, 50% and 20%. In this case, 80% SoC at 0.5C rate values has been used for all the calculations. Fig.3.5 is the voltage plot, and Fig.3.4 is the current plot of NMC 37 Ah used to calculate internal resistance.

$$SoH_{IR} = \frac{Measured_{IR}\ \sout{in\ each\ round}}{BoL_{IR}} * 100\%. \tag{3.2}$$

The equation 3.2 calculates the SoH_{IR} where the internal resistance at each round is calculated based on 2.1 in which V_1 and V_2 are the instantaneous voltage between two points with a time difference of 10 Sec. I is the current measured at the C/2 rate. Table 3.3 shows the calculated internal resistance value over different rounds. Later for plotting the graphs, rounds were converted into equivalent cycles.

Rounds	NMC 50Ah	NMC 43Ah	NMC 40Ah	NMC 37Ah	NMC 60Ah
0	100.00	100.00	100.00	100.00	100.00
1	101.62	96.84	105.09	99.09	110.43
2	103.24	96.39	101.65	108.18	116.86
3	103.24	97.07	100.90	105.45	115.07
4	99.03	92.10	98.50	114.09	122.64
5	100.97	90.97	94.31	115.45	165.10
6	101.62	93.00	93.41	121.82	
7	99.68		93.11	137.27	
8	100.65		88.02		
9	100.65		87.72		
10	100.65		88.32		
11	99.68		87.72		

Table 3.3: SoH_{IR} variation concerning rounds

From fig. 3.6, it can be seen that high power-density optimised cells have lower internal resistance than high energy-density cells. In the case of the latter, except NMC-43 Ah, after the elbow point, the internal resistance increases sharply. Because of test failure, the full equivalent cycle numbers of NMC-43 Ah were close by, so the results are inaccurate. For all other cells, there is a sufficient gap between the full equivalent cycles implying a successful test. In the case of NMC 37 Ah and NMC 60 Ah, there is an increase in SoH_{IR} with rounds, whereas for NMC 40 Ah, the SoH_{IR} decreases with rounds. However, in NMC 50 Ah, there is very little variation of SoH_{IR} with rounds.
The reason why high power-density optimised cells have lower internal resistance than high energy-density cells is the same as why the former has a higher capacity. After all, capacity and internal resistance are inversely proportional, as higher capacity results from lower internal resistance [29].

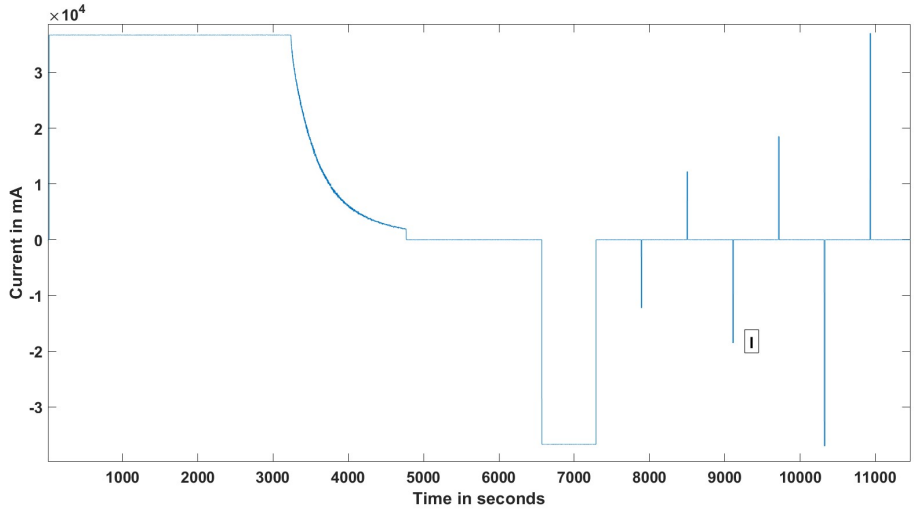

Figure 3.4: Current plot of NMC 37 Ah used for calculation of internal resistance

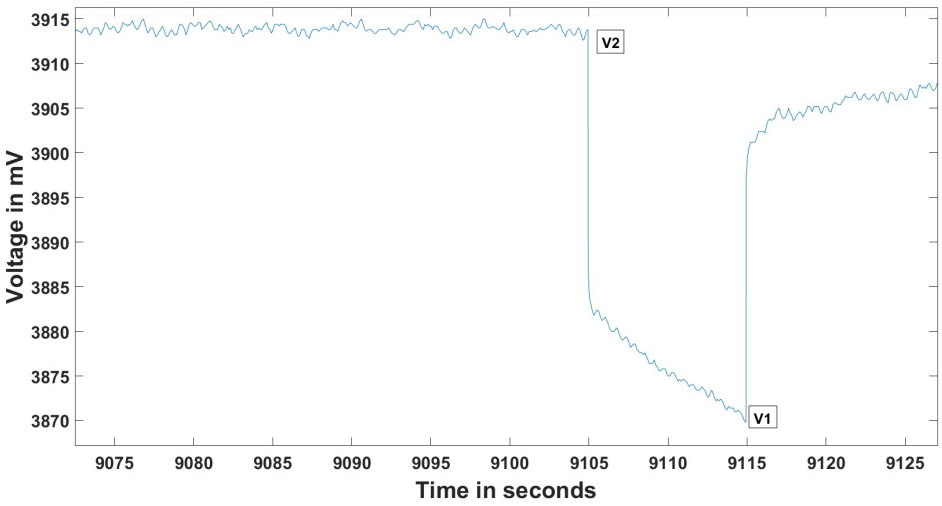

Figure 3.5: Voltage plot of NMC 37 Ah used for calculation of internal resistance

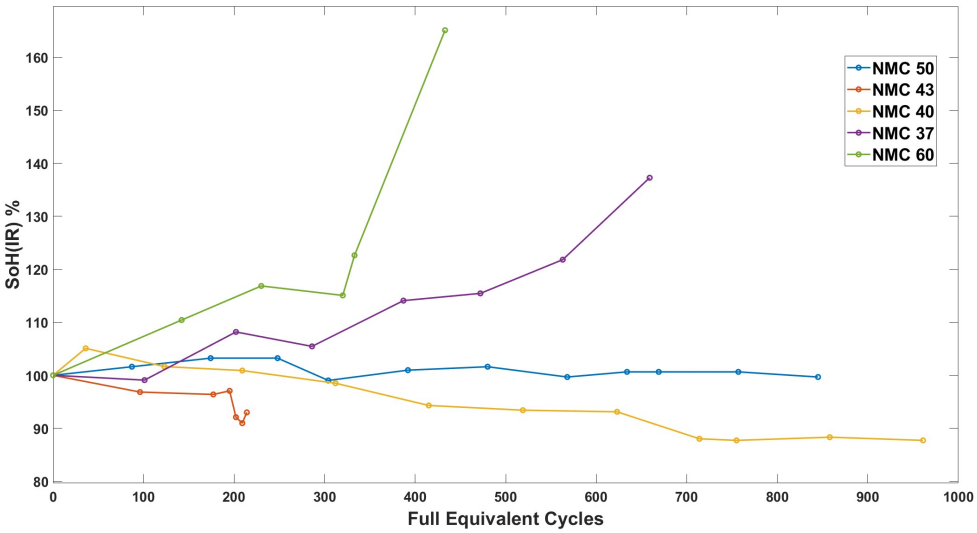

Figure 3.6: SoH_{IR} in different cells

3.3 Analysis on the rate of change of capacity and internal resistance

Graphs from fig.3.7 to fig.3.11 depict the rate of change (in percentage) of both internal resistance and capacity with respect to the previous round. In principle, capacity is expected to decrease with increased internal resistance. However, there could also be various reasons why this may not turn out to be accurate at all times. This is because due to complex mechanisms involving a combination of factors such as ageing, internal temperature and cycle life, both capacity and internal resistance exhibit a non-linear behaviour — next, looking at each case individually.

3.3.1 Comparison of NMC 37Ah

Fig. 3.7 is the plot comparing the rate of change of resistance and capacity of NMC 37Ah. Among 7 rounds, 5 rounds are such that when the rate of increase of capacity is opposite that of internal resistance. The capacity decreases from round 1 onwards. In this case, it takes 659 FECs to complete 7 rounds.

3.3.2 Comparison of NMC 40Ah

Fig. 3.8 is the plot comparing the rate of change of resistance and capacity of NMC 40 Ah. These cells have the highest FEC number of 961 to finish all the 11 rounds. Among 11 rounds, 5 rounds are such that when the rate of increase of capacity is opposite that of internal resistance.

3.3.3 Comparison of NMC 43Ah

Fig. 3.9 is the plot comparing the rate of change of resistance and capacity of NMC 43 Ah. Among 6 rounds, just two rounds are such that when the capacity increase is opposite of internal

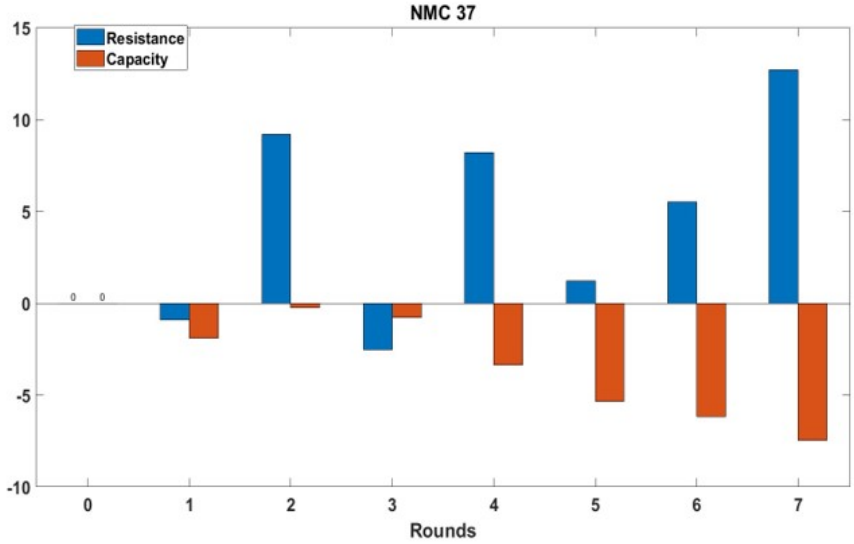

Rounds	FEC
0	0
1	101
2	202
3	286
4	387
5	472
6	563
7	659

Figure 3.7: Comparison of NMC 37Ah

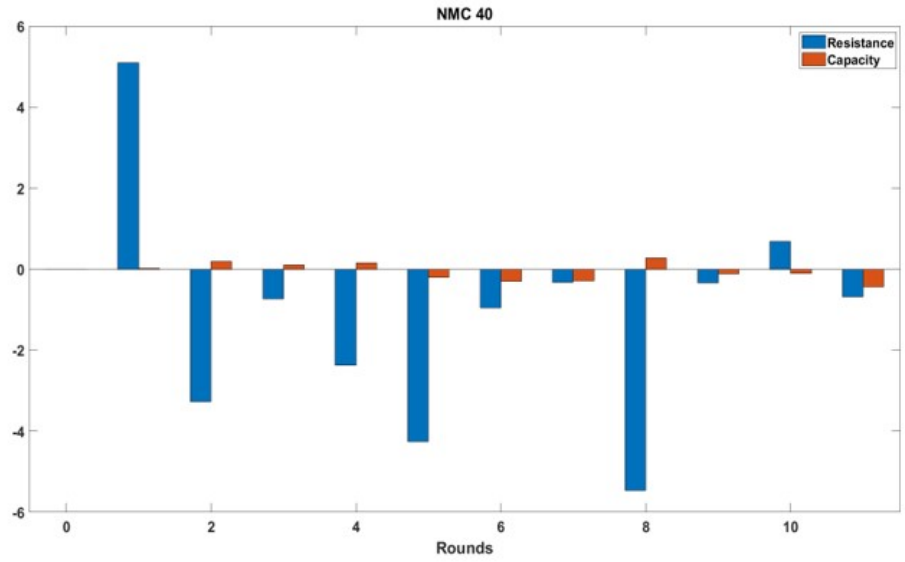

Rounds	FEC
0	0
1	36
2	123
3	209
4	312
5	415
6	519
7	623
8	714
9	755
10	858
11	961

Figure 3.8: Comparison of NMC 40Ah

resistance. The capacity decreases from round 1 onwards. Since the test was not successful, FEC number of the last round was just 214 with just 5 FEC between the last two rounds.

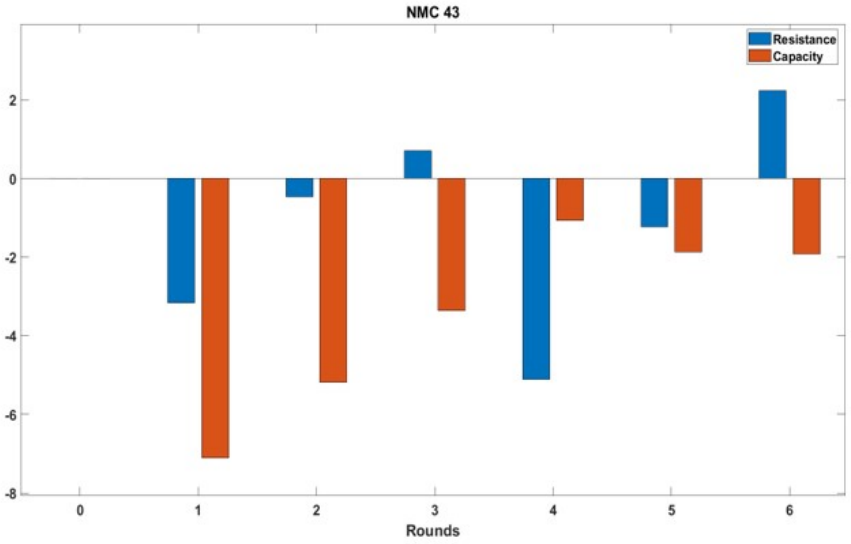

Rounds	FEC
0	0
1	96
2	177
3	195
4	202
5	209
6	214

Figure 3.9: Comparison of NMC 43Ah

3.3.4 Comparison of NMC 60Ah

Fig. 3.10 is the plot comparing the rate of change of resistance and capacity of NMC 60 Ah. Among 5 rounds, 4 rounds are such that when the capacity increase is opposite of internal resistance. The capacity decreases from round 1 onwards. FEC number after the last round is 433.

3.3.5 Comparison of NMC 50Ah

Fig. 3.11 is the plot comparing the rate of change of resistance and capacity of NMC 50 Ah. The experiment continues for 11 rounds with the FEC number at the end being 845. Among 11 rounds, 6 rounds are such that when the capacity increase is opposite of internal resistance. The capacity decreases from round 1 onwards

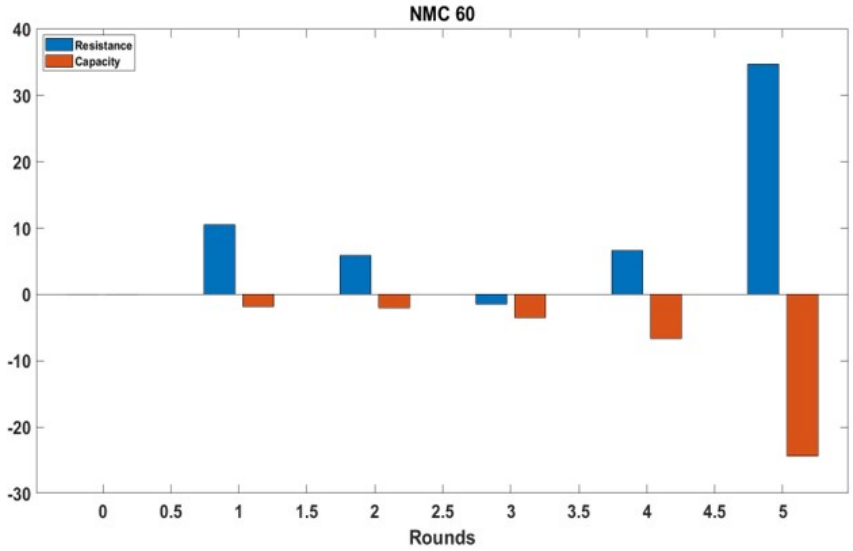

Rounds	FEC
0	0
1	142
2	230
3	320
4	333
5	433

Figure 3.10: Comparison of NMC 60Ah

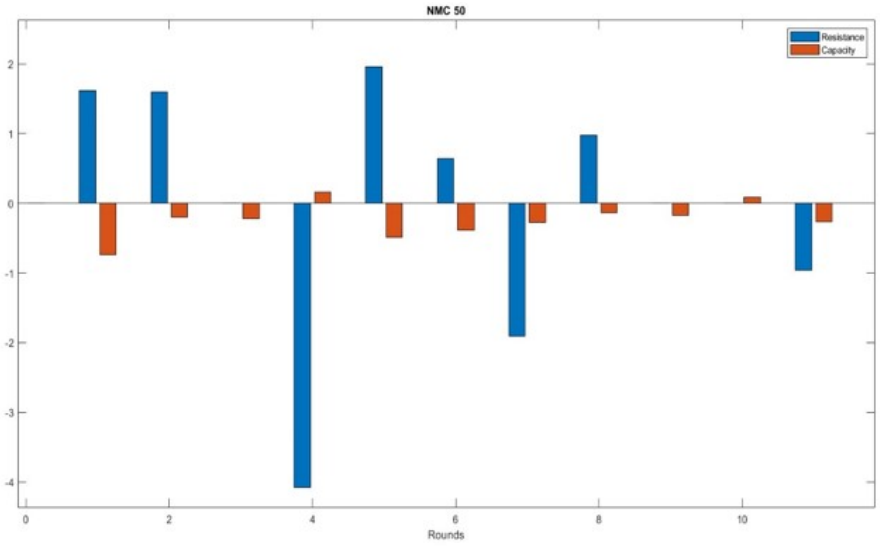

Rounds	FEC
0	0
1	87
2	174
3	248
4	304
5	392
6	480
7	568
8	634
9	669
10	757
11	845

Figure 3.11: Comparison of NMC 50Ah

3.3.6 General inference

It can be seen that, in all cases except 40 Ah, the capacity decreases after round 1. Batteries with high energy-density cells have fewer rounds than high power-density optimised cells. Also, the former has an elbow and knee point. Interestingly, high energy-density cells have more rounds where capacity and internal resistance show an inverse relation except NMC 43 Ah, which has a test set-up failure.
In a study, it has been observed that there is a correlation (called Pearson correlation) between internal resistance and capacity, which varies with the number of cycles, SoC, and temperature. For instance, the value of the Pearson coefficient is positive when the cycling begins, then becomes zero after 150 to 200 cycles. Eventually, after further cycles, it takes a negative value. [29].
In this experiment, the five different batteries are all from different manufacturers despite having the same chemistry. Also, the cell structure and capacity are different. This is perhaps why the correlation between internal resistance and capacity in the graphs differs for each battery, even though they are carried out under the same temperature and charging/discharging rate.

Chapter 4

Curve Fitting

Curve fitting is a method of forming an equation that best fits a set of data points. With respect to this experiment, the data points are variations in internal resistance and capacity with respect to the number of cycles. There are two main ways to attain curve fitting - one is interpolation and the other is smoothing. In interpolation, in between unknown values are estimated based on already known data points. In smoothing, the method is to create a formula that approximately fits the pattern exhibited by most of the points. In this experiment, smoothing is used. A fourth-order polynomial is created as in equation 4.1, where y is the unknown variable which is either internal resistance or capacity and x is the cycle number and a,b,c,d and e are the constants. These constants are solved and found since there are five constants and data sets from 5 battery sets. First, curve fitting was done in Microsoft Excel and then verified using MATLAB curve fitting toolbox.

$$y = ax^4 + bx^3 + cx^2 + dx + e \tag{4.1}$$

To know how well the curve fitting turned out to be, R^2 value is used which is a parameter to assess how good the fit is. The range of R^2 is between 0 and 1. An R^2 value of 0 implies that the curve does not fit at all, whereas an R^2 value of 1 implies that the curve fits through all points. R^2 is not a square of any parameter; it is basically a fraction of the total variance of the unknown variable, which is determined by the equation created to fit the data [30].

4.1 Capacity fitting

Table 4.1 is a table containing values of constants a to e and R^2 based on the curve fitting shown in figures 4.1 to 4.5 to determine the value of SoH based on capacity. It can be seen that the R^2 value is really good for all batteries except for NMC 40 Ah for which it is moderately good.

Battery	a	b	c	d	e	R^2
NMC40 Ah	-1.30E-11	2.78E-08	-2.10E-05	0.005494	99.9	0.8608
NMC50 Ah	2.43E-11	-4.07E-08	2.27E-05	-0.00768	99.93	0.9773
NMC60 Ah	-1.36E-09	4.87E-09	0.000136	-0.02965	100	0.9872
NMC43 Ah	-2.31E-08	5.96E-06	-0.00022	-0.08749	100	0.9994
NMC37 Ah	5.38E-10	-7.52E-07	0.000267	-0.03807	99.98	0.9995

Table 4.1: Value of constants for SoH_{Cap} fit

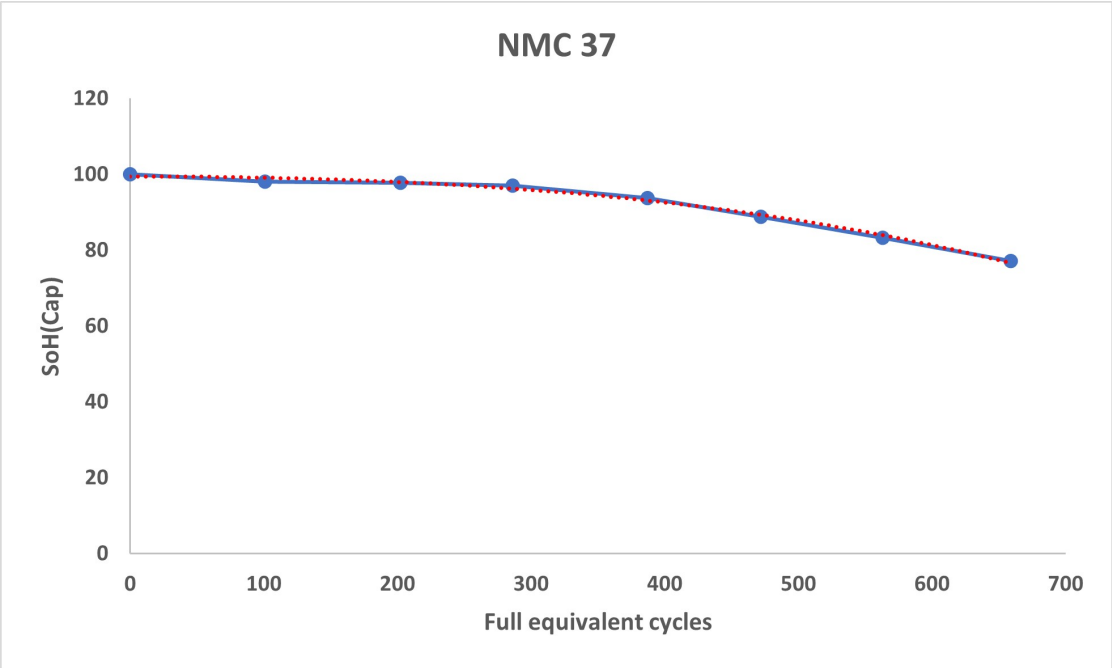

Figure 4.1: Curve fitting of NMC 37Ah-SoH_{Cap}

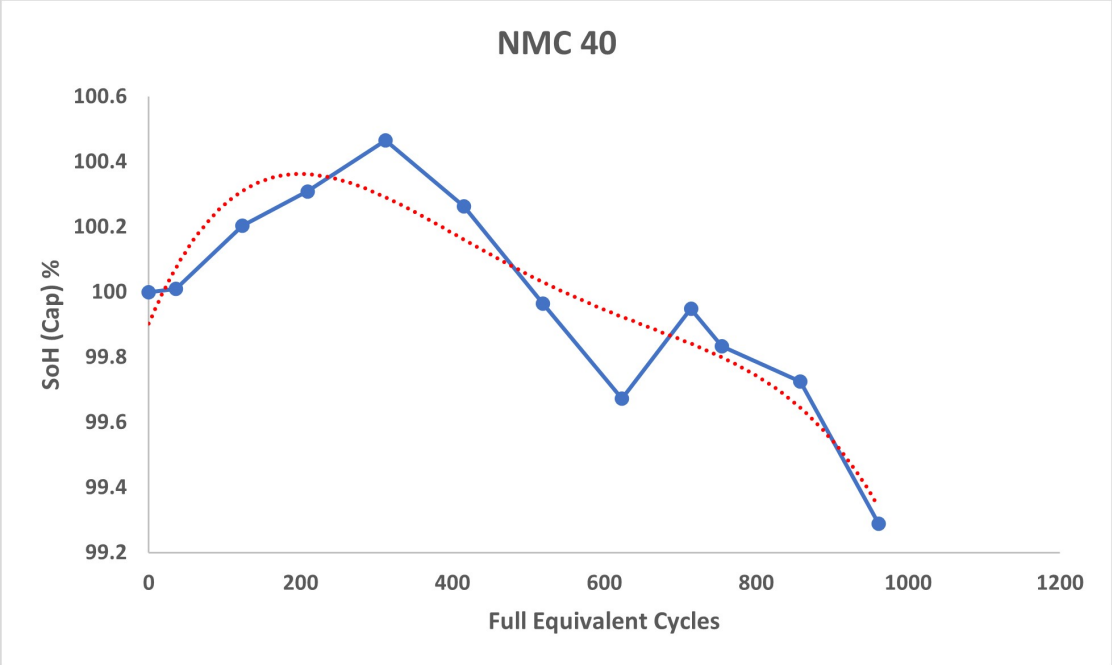

Figure 4.2: Curve fitting of NMC 4OAh-SoH_{Cap}

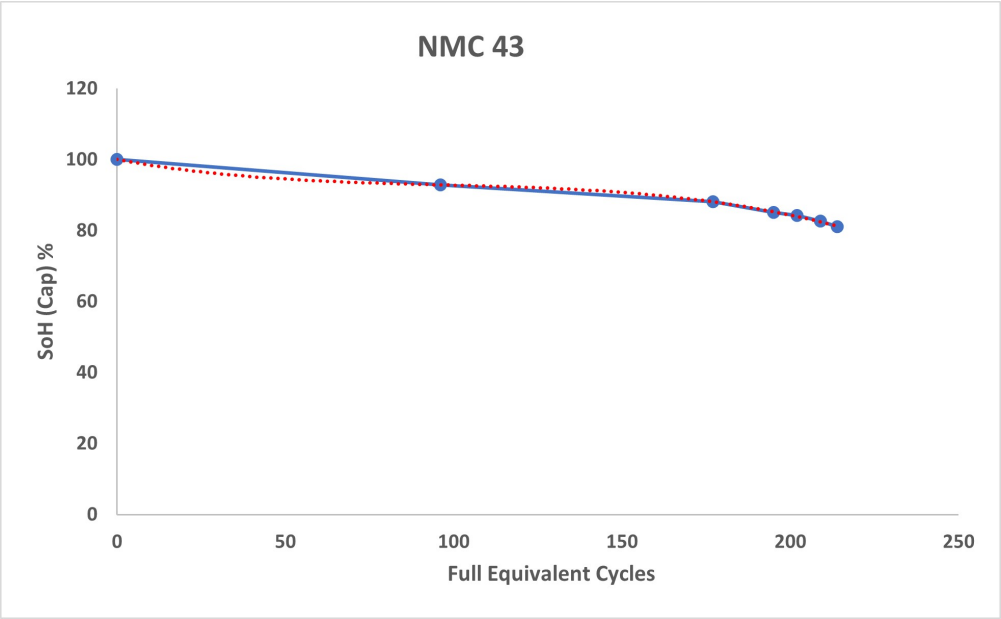

Figure 4.3: Curve fitting of NMC 43Ah-SoH_{Cap}

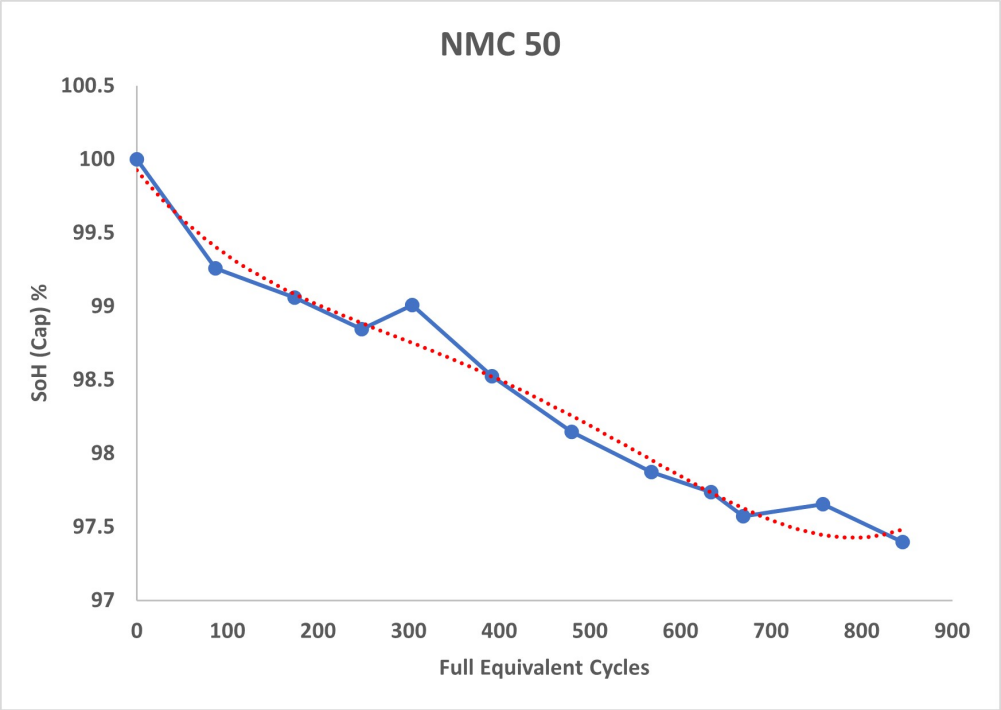

Figure 4.4: Curve fitting of NMC 5OAh-SoH_{Cap}

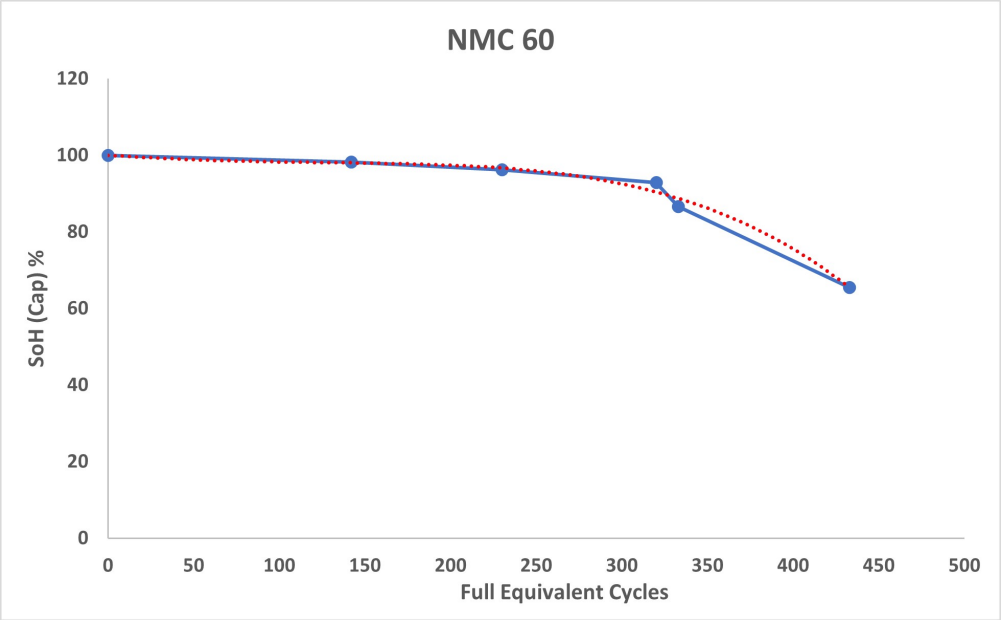

Figure 4.5: Curve fitting of NMC 6OAh-SoH_{Cap}

Battery	a	b	c	d	e	R^2
NMC40 Ah	-5.87E-11	1.61E-07	-1.34E-04	0.01683	101.9	0.9477
NMC50 Ah	-1.81E-10	3.34E-07	-2.01E-04	0.04033	99.93	0.4558
NMC60 Ah	1.83E-08	-1.32E-05	0.002934	-0.1274	99.98	0.9924
NMC43 Ah	5.71E-08	-3.44E-05	0.006289	-0.3708	100	0.8023
NMC37 Ah	1.17E-09	-1.35E-06	0.000518	-0.03354	99.76	0.9765

Table 4.2: Value of constants for SoH_{IR} fit

4.2 Internal resistance fitting

Table 4.2 is a table containing values of constants a to e and R^2 based on the curve fitting shown in figures 4.6 to 4.10 to determine the value of SoH based on internal resistance. It can be seen that the R^2 value is really good for all batteries except for NMC 50 Ah for which it is not that good, and NMC 43 Ah, for which it is moderately good.

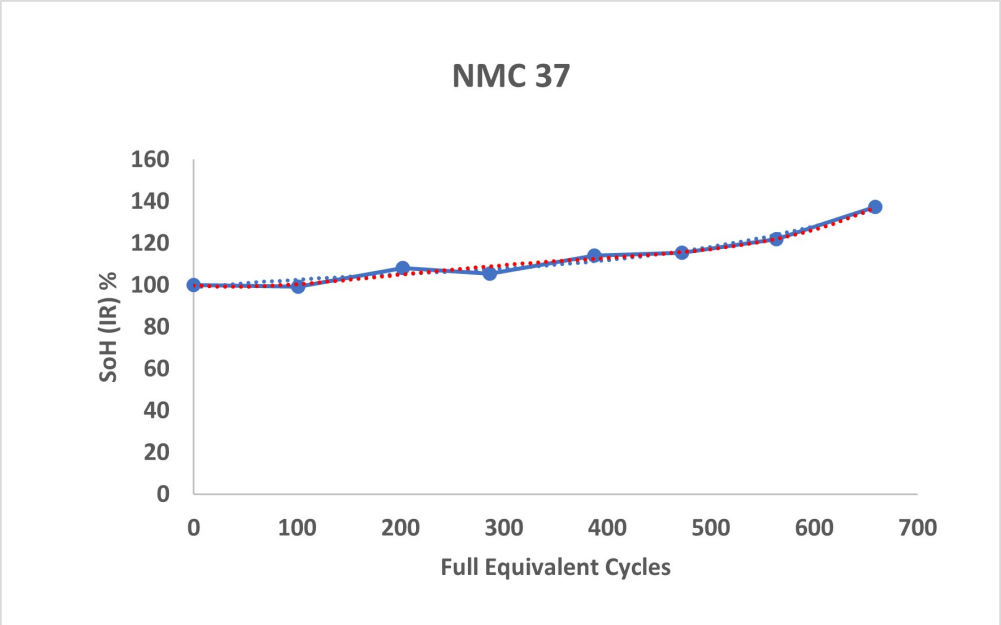

Figure 4.6: Curve fitting of NMC 37Ah-SoH_{IR}

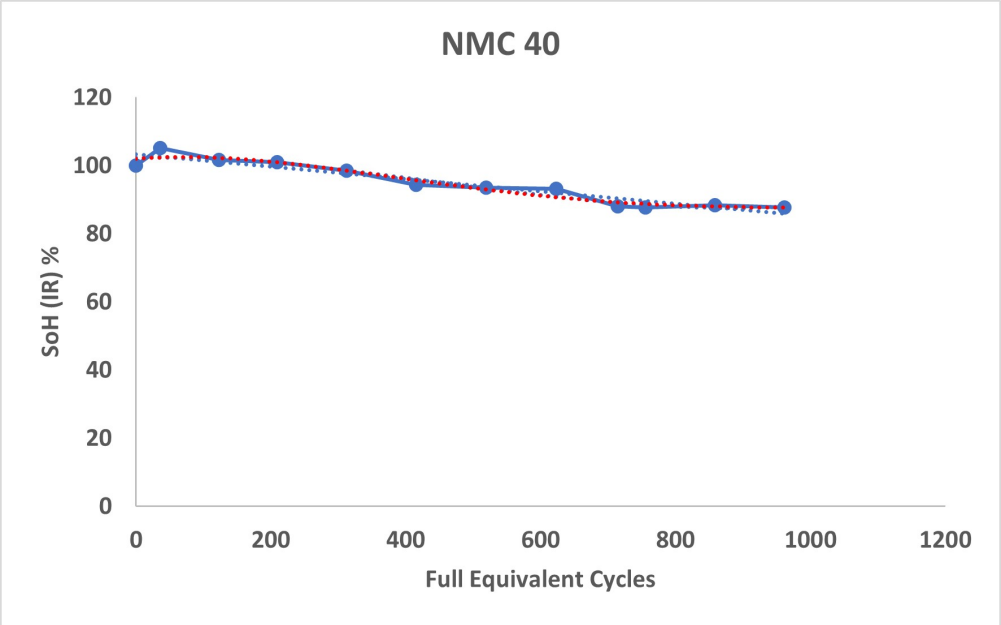

Figure 4.7: Curve fitting of NMC 4OAh-SoH_{IR}

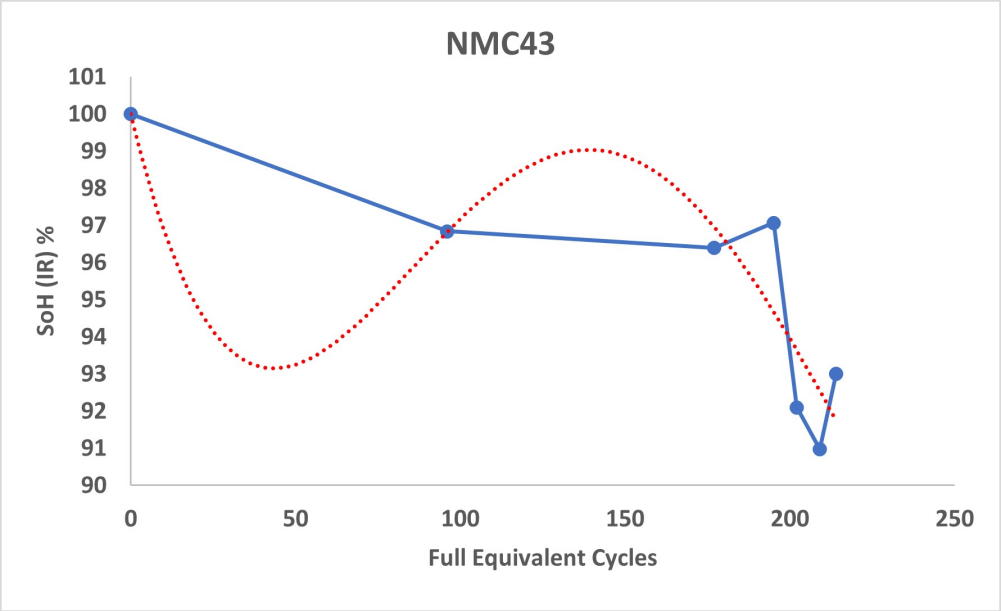

Figure 4.8: Curve fitting of NMC 43Ah-SoH_{IR}

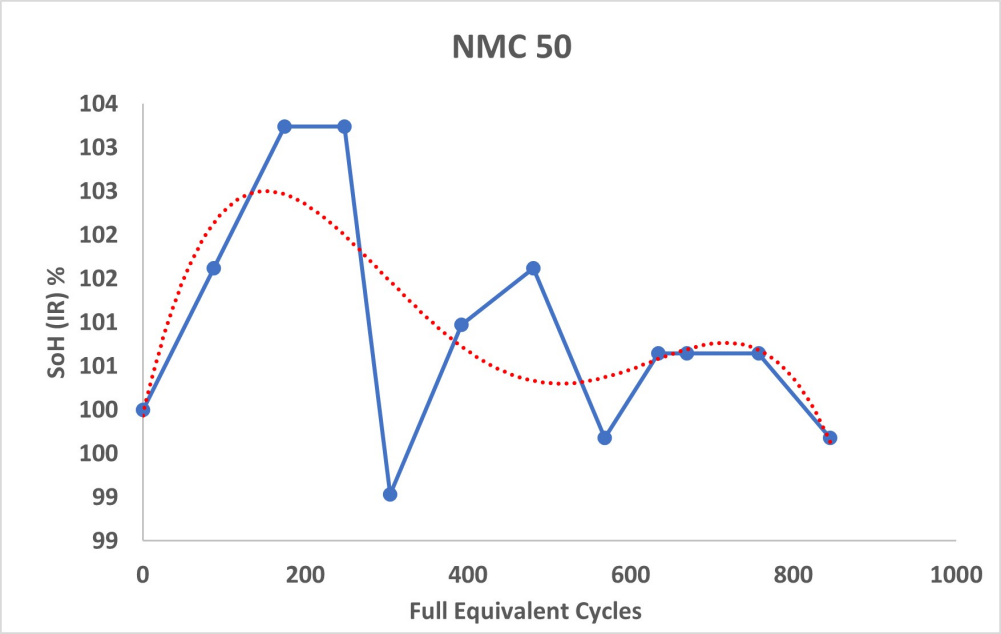

Figure 4.9: Curve fitting of NMC 5OAh-SoH_{IR}

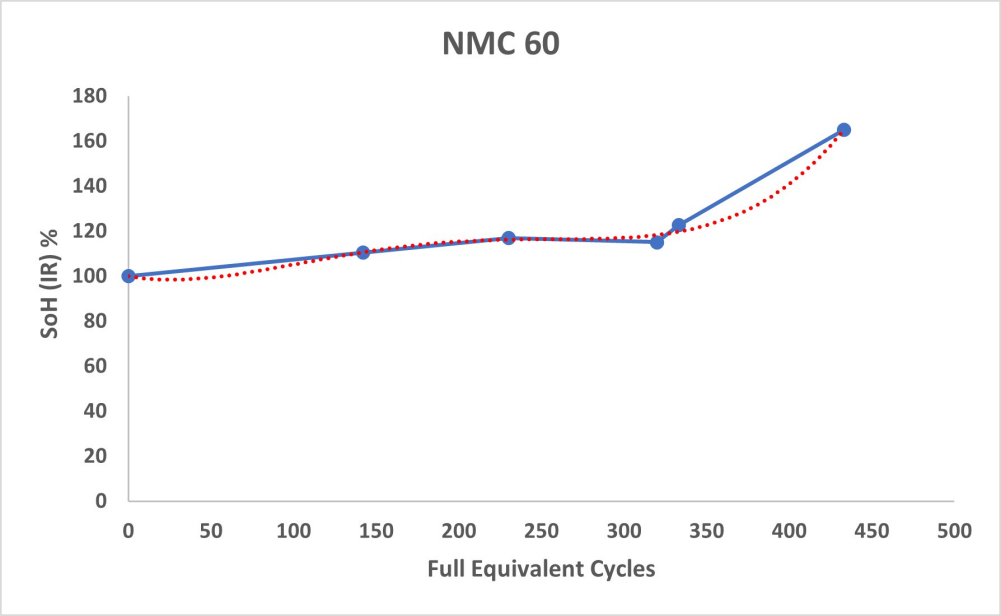

Figure 4.10: Curve fitting of NMC 60Ah-SoH_{IR}

4.3 Rationality of the study

In this study, since the hybrid testing methodology combining cycling and resting in a single round is used, the results can be used in real-life scenarios. Also since five different batteries are used, it is possible to understand the similarities and differences in the way battery cells age for each of the batteries. The main objective of the BMS system is to have control over the functioning of the battery. This includes observing parameters, predicting values, and also offering warnings. First, parameters such as temperature, battery voltage, and current are monitored. The estimation of internal resistance and capacity follows this. Since this curve fitting method involves fourth-order polynomials which are equations, it can be programmed into the microcontroller of the chip used in BMS. For this, an algorithm in the form of a flow chart is made to implement this new formula as a program. Then a program is written as per the flow chart in a language suitable for the microchip. The equation and its coefficients are known for a given battery type. Thus by enabling this function of BMS control, it is possible to estimate the capacity and internal resistance of the battery for a different number of cycle numbers. Using this information, it is possible to know in advance the remaining lifetime of the battery.

Chapter 5

Conclusion, Limitation & Future work

5.1 Conclusion

In this thesis, five different NMC commercial Li-ion batteries – 37 Ah, 40 Ah, 43 Ah, 60 Ah and 50 Ah are investigated. A hybrid testing method where one round comprises cycling and resting is followed to resemble practical application. HPPC test, capacity test and WLTC test cycle are used for the experiment subject to other constraints such temperature, C rate and SoC as described in chapter 2. The results from the experiment are gathered and analyzed to observe the behavior of internal resistance and capacity with cycle number, as shown in 3. The experiment was successfully carried out for five batteries with 43 Ah experiencing a performance failure towards its end of life. Based on the analysis, it can be concluded that there is indeed a correlation between internal resistance and capacity. However, this correlation is not the same for all the five batteries.

Once the data is analysed, a fourth-order polynomial equation using the curve fitting method in Microsoft Excel is used to model the parameters described in 4. The unknown variables to be solved are the SoH based on internal resistance and the capacity (which are also the key parameters that determine the degradation of the battery). Considering that the fourth-order polynomial has five unknowns and that there are five battery types, these coefficients are solved, thus completing the model. MATLAB is then used to validate the model. R^2 value is used to check how closely the fit is. It can be concluded from the values of R^2 that the constructed formula closely matches the data obtained from the experiment, and hence the model is reasonably good.

Overall as described in section 3.3.6, it can be inferred from this thesis that there is a correlation between internal resistance and capacity, which vary according to the battery chemistry. It can be concluded that using curve fitting – a proposed formula with different coefficients for each battery chemistry, an accurate model can be created to estimate internal resistance and capacity.

Thus using a hybrid test set-up, data analysis and curve fitting, a good model to estimate battery ageing has been proposed.

5.2 Limitation

In Lithium-ion batteries, capacity loss and internal resistance growth, are a consequence of many internal and external factors, some of which are temperature, mechanical stress, current rate, depth of discharge etc. This experimental setup cannot specify the exact reason behind the internal resistance growth and capacity fade. Here all five cells are tested through a similar experimental method where the temperatures used are 10°C and 25 °C, and the used charging and discharging rate was also limited; hence it is tough to point out the specific reason behind the battery degradation. If the test has been carried out under different temperature ranges and through different C rates, then it will be easy to do broader studies by comparing the results obtained. Additionally, there could be limitations to using curve fitting as it is fundamentally a tool that uses approximation. This can result in potential errors in the model. Already in this thesis, it was seen that though the R^2 value is good in four cases, it is poor in one case.

5.3 Future work

As an extension of this work, the experimental data used in this experiment can be used to train an artificial neural network (ANN) model, which will be highly capable of predicting the results more accurately. ANN has an excellent capacity to learn the intricate correlation between input and output based on a minimal data set. Subjecting the experiment set-up to a wider range of operating conditions, such as more temperature settings and larger C rates, will enable the formulation of a more precise model.

Bibliography

[1] Md Sazzad Hosen, Danial Karimi, Theodoros Kalogiannis, Ashkan Pirooz, Joris Jaguemont, Maitane Berecibar, Joeri Van Mierlo, "Electro-aging model development of nickel-manganese-cobalt lithium-ion technology validated with light and heavy-duty real-life profiles", Journal of Energy Storage, Volume 28, 2020, 101265, ISSN 2352-152X, :https://doi.org/10.1016/j.est.2020.101265

[2] Armin Razmjoo, Arezoo Ghazanfari, Mehdi Jahangiri, Evan Franklin, Mouloud Denai, Mousa Marzband, Davide Astiaso Garcia and Alireza Maheri, "A Comprehensive Study on the Expansion of Electric Vehicles in Europe", Applied Sciences, 2022; 12(22):11656, :https://doi.org/10.3390/app122211656

[3] Dominic A. Notter, Marcel Gauch, Rolf Widmer, Patrick Wäger, Anna Stamp, Rainer Zah, and Hans-Jörg Althaus "Contribution of Li-Ion Batteries to the Environmental Impact of Electric Vehicles", Environ. Sci. Technol. 2010, 44, 17, 6550–6556 Applied Sciences. Aug 2010; 12(22):11656, :https://doi.org/10.1021/es903729a

[4] Rui Martim Salgado, Federico Danzi, Joana Espain Oliveira, Anter El-Azab, Pedro Ponces Camanho and Maria Helena Braga, "The Latest Trends in Electric Vehicles Batteries", The Latest Trends in Electric Vehicles Batteries. Molecules, 2021, 26, 3188. : https://doi.org/10.3390/molecules26113188

[5] UL Research Institutes, Electrochemical Safety Research Institute, What Are Lithium-Ion Batteries, September 14, 2021 https://ul.org/research/electrochemical-safety/getting-started-electrochemical-safety/what-are-lithium-ion (Accessed Apr. 30, 2023)

[6] Battery University, BU-105: Battery Definitions and what they mean https://batteryuniversity.com/article/bu-105-battery-definitions-and-what-they-meanhttps://batteryuniversity.com/article/bu-105-battery-definitions-and-what-they-mean (Accessed Apr. 23, 2023)

[7] The International Council on Clean Transportation: A global comparison of the life-cycle greenhouse gas emissions of combustion engine and electric passenger cars https://theicct.org/publication/a-global-comparison-of-the-life-cycle-greenhouse-gas-emissions-of-combustion/-engine-and-electric-passenger-cars/ (Accessed Apr. 23, 2023)

[8] Battery University, BU-908: Battery Management System (BMS) https://batteryuniversity.com/article/bu-908-battery-management-system-bms (Accessed Apr. 23, 2023)

[9] Battery University, BU-808b: What Causes Li-ion to Die? https://batteryuniversity.com/article/bu-808b-what-causes-li-ion-to-die (Accessed Apr. 23, 2023)

[10] Rui Xiong, Yue Pan, Weixiang Shen, Hailong Li, Fengchun Sun, "Lithium-ion battery aging mechanisms and diagnosis method for automotive applications: Recent advances and perspectives", Renewable and Sustainable Energy Reviews, Volume 131, 2020, 110048, ISSN 1364-0321, :https://doi.org/10.1016/j.rser.2020.110048.

[11] Agubra, V., Fergus, J., "Lithium Ion Battery Anode Aging Mechanisms. Materials", Renewable and Sustainable Energy Reviews, Volume 131, 2020, 110048, 2013, Materials, 6(4), 1310-1325, :https://doi.org/10.3390/ma6041310

[12] Eduardo Redondo-Iglesias, Pascal Venet, Serge Pelissier, "Calendar and cycling ageing combination of batteries in electric vehicles", Renewable and Sustainable Energy Reviews, Volumes 88–90, 2018, Pages 1212-1215, ISSN 0026-2714, :https://doi.org/10.1016/j.microrel.2018.06.113.

[13] M. Tutuianu, A. Marotta, H. Steven, E. Ericsson, T. Haniu, N. Ichikawa, H. Ishii, "Development of a World-wide Worldwide harmonised Light duty driving Test Cycle (WLTC)", Technical Report, DHC subgroup, 03 (2014) 7–10. Webpage, (2020). :https://unece.org/fileadmin/DAM/trans/doc/2014/wp29grpe/GRPE-68-03e.pdf(Accessed Apr. 27, 2023)

[14] Md Sazzad Hosen, Rekabra Youssef, Theodoros Kalogiannis, Joeri Van Mierlo, Maitane Berecibar, "Battery cycle life study through relaxation and forecasting the lifetime via machine learning", Volume 40, 2021, 102726, ISSN 2352-152X, :https://doi.org/10.1016/j.est.2021.102726.

[15] Md Sazzad Hosen, Theodoros Kalogiannis, Rekabra Youssef, Danial Karimi, Hamidreza Behi, Lu Jin, Joeri Van Mierlo, Maitane Berecibar, "Twin-model framework development for a comprehensive battery lifetime prediction validated with a realistic driving profile", Energy Science and Engineering, 9(11), 2191-2201, (2021), :https://doi.org/10.1002/ese3.973

[16] Keshavarzi Mohammad, Derakhshan Mohsen, Gilaki Mehdi, L'Eplattenier Pierre, Çaldichoury Iñaki, Soudbakhsh Damoon, Sahraei Elham, "Coupled Electrochemical-Mechanical Modeling of Lithium-Ion Batteries Using Distributed Randle Circuit Model", Energy Sci Eng. 2021;9:2191–2201,Conference: 2021 International Conference on Electrical, Computer and Energy Technologies (ICECET) :https://doi.org/10.1109/ICECET52533.2021.9698796

[17] Battery Design from chemistry to pack, Open Circuit Voltage
https://www.batterydesign.net/electrical/open-circuit-voltage/
(Accessed Apr. 29, 2023)

[18] ROHM SEMICONDUCTOR, Charging Method
https://www.rohm.com/electronics-basics/battery-charge/charging-method
(Accessed Apr. 29, 2023)

[19] MathWorks, Help Center, Battery CC-CV,
https://nl.mathworks.com/help/simscape-battery/ref/batterycccv.html
(Accessed Apr. 29, 2023)

[20] Owlcation, A Simple Comparison of Six Lithium-Ion Battery Types, CHARLES NUAMAH, FEB 17, 2023
https://owlcation.com/stem/Comparing-6-Lithium-ion-Battery-Types
(Accessed Apr. 30, 2023)

[21] Alexandra K. Stephan, "A Pathway to Understand NMC Cathodes", Joule 4, 1626–1636, August 19, 2020, :https://doi.org/10.1016/j.joule.2020.08.004

[22] electronicnotes, Battery Definitions, Terms and Terminology, https://www.electronics-notes.com/articles/electronic_components/battery-technology/terms-terminology-definitions.php (Accessed Apr. 30, 2023)

[23] Mewburn Ellis, Increasing battery capacity: going Si high, 24 June 2020 https://www.mewburn.com/news-insights/increasing-battery-capacity-going-si-high (Accessed Apr. 30, 2023)

[24] Houache, Mohamed S. E., Chae-Ho Yim, Zouina Karkar, and Yaser Abu-Lebdeh., "On the Current and Future Outlook of Battery Chemistries for Electric Vehicles—Mini Review", Batteries 8, no. 7: 70., 2022, :https://doi.org/10.3390/batteries8070070

[25] Li Dongjiang, Danilov Dmitri, Bergveld H, Eichel Rüdiger-A, Notten Peter, "CHAPTER 9: Understanding battery aging mechanisms.", Future Lithium-ion Batteries, 2019, :http://dx.doi.org/10.1039/9781788016124-00220

[26] UNIVERSITY OF CAMBRIDGE, Battery characteristics, 24 June 2020 https://www.doitpoms.ac.uk/tlplib/batteries/battery_characteristics.php (Accessed May 1, 2023)

[27] BioLogic, Battery states: State of charge (SoC), State of Health (SoH). Electrochemistry basics series., February 8, 2023 https://www.biologic.net/topics/battery-states-state-of-charge-soc-state-of-health-soh/ (Accessed May 5, 2023)

[28] Battery Design from chemistry to pack, Power versus Energy Cells, Nigel, January 14, 2022 https://www.batterydesign.net/power-versus-energy-cells/ (Accessed May 18, 2023)

[29] Mohammad A. Hoque, Petteri Nurmi, Arjun Kumar, Samu Varjonen, Junehwa Song, Michael G. Pecht, Sasu Tarkoma, "Data driven analysis of lithium-ion battery internal resistance towards reliable state of health prediction", Journal of Power Sources, Volume 513, 2021, 230519, ISSN 0378-7753, https://doi.org/10.1016/j.jpowsour.2021.230519.

[30] GraphPad, R squared, https://www.graphpad.com/guides/prism/latest/curve-fitting/reg_intepretingnonlinr2.htm (Accessed May 21, 2023)

[31] Rui Xiong, Yue Pan, Weixiang Shen, Hailong Li, Fengchun Sun, "Lithium-ion battery aging mechanisms and diagnosis method for automotive applications: Recent advances and perspectives", JoRenewable and Sustainable Energy Reviews, Volume 131, 2020, 110048, ISSN 1364-0321, https://doi.org/10.1016/j.rser.2020.110048.

[32] Battery capacity testing: what it is, how it works, and why you should be doing it., February 25, 2022 https://www.bestmag.co.uk/battery-capacity-testing-what-it-is-how-it-works-and-why-you-should-be-doing-it/ (Accessed May 23, 2023)

[33] Jian Ma, Shu Xu, Pengchao Shang, Yu ding, Weili Qin, Yujie Cheng, Chen Lu, Yuzhuan Su, Jin Chong, Haizu Jin, Yongshou Lin, "Cycle life test optimization for different Li-ion power battery formulations using a hybrid remaining-useful-life prediction method", Applied Energy, Volume 262, 2020, 114490, ISSN 0306-2619, https://www.sciencedirect.com/science/article/pii/S0306261920300027

[34] Project HELIOS - High Energy Lithium-Ion Storage Solutions., Initial cycling and calendar ageing test procedures and checkup tests for high energy Li-ion battery cells, Novemeber 2011 https://trimis.ec.europa.eu/sites/default/files/project/documents/20120404_144903_76248_HELIOS_DELIVERABLE_3_2.pdf (Accessed May 23, 2023)

[35] Derek Heeger, Mike Partridge, Von Trullinger, Dan Wesolowski, "Lithium Battery Health and Capacity Estimation Techniques Using Embedded Electronics", Sandia Report, October 2017

[36] Suyeon Sohn, Ha-Eun Byun, Jay H. Lee, "Two-stage deep learning for online prediction of knee-point in Li-ion battery capacity degradation", Applied Energy, Volume 328, 2022, 120204, ISSN 0306-2619, https://www.sciencedirect.com/science/article/pii/S0306261922014611

[37] Lithium-Ion Battery Management Systems and large battery packs-Directories and resources for engineers and users.http://liionbms.com/pdf/kokam/SLPB100216216H.pdf(Accessed May 30, 2023)

[38] "Cell specification of CATL 50Ah NMC Lithium battery "- Data sheet